Pleistocene precipitation changes using O and C isotopes on a speleothem from the Majuanas Cave System, Cuba

Mercedes Liedtke

Supervisors

Dr. Matthew Peros

Dr. André Viau

A thesis submitted in partial fulfillment for the requirements of a Master of Science degree in Geography.

University of Ottawa

Department of Geography, Environment and Geomatics

Abstract

A stalagmite was collected in the Salón de la Permencia of the Majaguas Cave, that is a part of the Majaguas-Cantera Cave System in Cuba. The use of this stalagmite as a natural climate archive is advantageous not only because stalagmites can record continuous episodes of growth that are thousands of years in duration but also because they are easily and reliably dated, using U/Th dating methods. With this method, the stalagmite was reliably dated to 100 ka and was still active when removed from the cave for analysis. The stable isotopes of oxygen and carbon from this stalagmite from Western Cuba presents information of significant influencing factors on Caribbean precipitation records, and past climatic events during the Pleistocene. Due to the lack of high-resolution records for Western Cuba, this study verifies and adds to our knowledge of past climate variability for the Cuban region and the Caribbean as a whole. The $\delta^{18}O$ data in MCS-01 shows a pattern that is very similar to the D-O and Heinrich events clearly recorded in the NGRIP ice core, especially at ~82ka and between 78-70ka. This study provides a continuous precipitation record for the area during the Pleistocene, allowing a greater understanding of the climate drivers that have had an impact on past precipitation patterns in this region.

Acknowledgments

First, and most of all, I would like to thank Dr. Matthew Peros, for introducing me to the world of paleoclimatology. It was only due to his valuable guidance, cheerful enthusiasm and ever-friendly nature that I was able to complete this research. I am forever grateful for his expertise, assistance, guidance, and patience throughout the - seemingly never-ending - process of writing this thesis. Without your help and unwavering support this thesis would not have been possible.

I would also like to thank Dr. André Viau for the support, and tireless effort put in over the course of this thesis. Thank you for working to actively provide me with the academic time to pursue my goals. I would like to thank my committee members, Dr. Ian Clark and Dr. Denis Lacelle, for their support, suggestions and encouragement.

To the Laboratory of Paleoclimatology and Climatology, I thank each and every one of you for your support and friendship. I feel privileged to have had the chance to meet all of you and could not imagine a more encouraging environment. . Thank you to Amanda, Michelle B, Paige, Michelle C, Karen, & Camille for all the laughs and the unwavering support. There are no other people I could have imagined sharing this journey with.

Nobody has been more important to me in the pursuit of this project than the members of my family. I would like to thank my parents, whose love and guidance are with me in whatever I pursue. They are the ultimate role models.

-M

Table of Contents

List of Tables

List of Figures

Chapter 1 - Introduction

The study of climate change through the Pleistocene to the present can contribute to a better understanding of the magnitude and rates of change of natural climate variability in the context of current global warming. Research on paleoclimates (ie. past climates) uses proxy climate archives in order to extend the historical observation record. These climate proxies are natural archives that include ice cores, sediment cores, tree rings, corals, or in the case of this study – speleothems.

Speleothems are secondary mineral deposits that are chemically precipitated in caves as calcium carbonate ($CaCO_3$). This precipitation is due to the process of chemical weathering that produces carbonate seepage waters (Hill and Forti, 2004). In the past few decades, growing interest in speleothems and their use as multi-proxy archives of climatic and environmental change has seen a surge in studies related to them. Speleothems are useful for paleoclimate reconstruction as the cave environment protects the speleothem, providing a stable environment for formation (Turgeon and Lundberg, 2007). As such, speleothems record important climate information that can be extracted though geochemical analyses. During the formation process of speleothems, trace elements and organic compounds are included from seepage waters, and these can reveal important information about the conditions under which the speleothem was formed (Frappier et al. 2007). Moreover, speleothem growth is sensitive to subtle changes occurring at the surface, such as variations in temperature, precipitation and vegetation; speleothems can then record these conditions at the time of their deposition (White 2007).

The Caribbean is a highly interesting study region, located in the subtropics, it is influenced by both Pacific and Atlantic oceanic and atmospheric processes (Fensterer,

2011). The competing influence of these modes of climate variability on tropical Atlantic climate is called the Tropical Atlantic Variability (TAV) (Fensterer, 2011). The Caribbean therefore represents an important area to obtain information about past natural climate variability in the tropics and its relationship to climate forcing mechanisms.

Climate change in the Caribbean region has also played an important role in local human history. For instance, episodes of severe drought in the Yucatan Peninsula are thought to have caused the collapse of the Maya Civilization, and paleoclimatic research using speleothems has been important at helping to define the timing, spatial extent, and severity of the droughts that occurred at this time (Fensterer et al. 2013a).

This study presents new results on Pleistocene precipitation changes using $\delta^{18}O$ and $\delta^{13}C$ isotopes over the last 100 ka on a speleothem from the Majuanas Cave System, Cuba.

1.1 Literature Review

1.1.1 Paleoclimate reconstructions in the tropics

Late Pleistocene:

One of the oldest paleoenvironmental records from the eastern equatorial Pacific Ocean is a sea surface salinity reconstruction that spans the past 90 000 years (Leduc et al. 2007). This record utilized a sediment core by comparing paleotemperature estimates from alkenones and Mg/Ca ratios along with foraminiferal oxygen isotope ratios, which vary due to both temperature and salinity. Millennial-scale fluctuations of sea surface salinities of up to two to four practical salinity units were detected. These high salinities are associated with the southward migration of the Intertropical Convergence Zone (ITCZ), coinciding with Henrich events (characterized large inputs of freshwater and ice-

rafted debris into the North Atlantic) and stadials (cold periods) recorded in Greenland ice cores. These paleotemperature records indicate that rapid climate change occurred on a millennial timescale during Marine Isotope Stage 3 (MIS 3) and these results were linked with the process of North Atlantic Deep Water (NADW) formation.

Another important study in the northeast Pacific Ocean from the Santa Barbara basin involved a record of ocean oxygenation and circulation that correlates well with the Greenland ice-cores (Behl and Kennett 1996). This study found that 19 of the 20 Dansgaard-Oeschger events (rapid, periodic swings in climate) are detected in the form of laminated sediments that were deposited under anoxic conditions (Behl and Kennett 1996). Of these, 16 events were correlated with 17 ice-core interstadials over the past 60 kyr. This study concluded that these events were not just restricted to the North Atlantic region and were more widespread than previously thought (Leduc et al. 2007). These events also had substantial ecological and oceanographic effects in the Santa Barbara basin, including influencing benthic faunal populations and the age and composition of ocean bottom waters (Behl and Kennett 1996).

Moving east to Lake Tulane, a sinkhole lake on Lake Wales Ridge in Florida – which formed through the dissolution of Eocene limestone - a pollen and plant macrofossil record from a core spanning the past 60 000 years was developed (Grimm et al. 2006). This record showed a strong anti-phase relationship in temperature between Florida and the North Atlantic region. In a previous study at the same location (Grimm et al. 1993), pollen analyses indicated possible coevality of *Pinus* peaks and Heinrich events, with five *Pinus* peaks correlating with H1-H5, and an extra *Pinus* peak occurring between H3 and H4. In this more recent study (Grimm et al. 2006), six *Pinus* peaks

correspond with H1-H6. Unfortunately, more precise correlation of the Lake Tulane pollen record with the Greenland $\delta^{18}O$ record is hampered by large errors in radiocarbon based chronology for the period older than 30 000 ^{14}CyrBP (Grimm et al. 2006).

In Central Mexico, Metcalfe et al. (2000) constructed a 35 000 year record of vegetation change. The Jalapasquillo series core was extracted from a Marr deposit in the State of Puebla and covers the Late Pleistocene to early Holocene (Metcalfe et al. 2000). The pollen record for the late Pleistocene was dominated by *Pinus* with some *Quercus, Picea* and *Alnus,* which are associated with colder and possibly wetter conditions than at present (Metcalfe et al., 2000; Brown, 1985). In another study from Mexico, isotopic and trace element (Mg/Ca and Sr/Ca) analyses of ostracods have been applied to cores from Lake Pátzcuaro and La Piscina de Yuriria. Records from La Piscina de Yuriria extend back 26 000 yrs, and suggest that in the late Pleistocene generally dry conditions are recorded at 26 000, 20 000, and then again between 19 000 and 14 700 yr BP (Metcalfe et al. 2000).

Building on this, Bradbury (1989) found that the terminal Pleistocene (14 000 – 10 000) was moist, but the early Holocene (9000-7000) was dry and warm (Metcalfe et al. 2000). This record provides a review of diatom data that was generated from the Basin of Mexico. Where, this study is comprised of data from five sites in the Texcoco and Chalco sub-basins and uses a chronology based on radiocarbon dates and tephras. This record also provides information that around 18 000 yr BP is seen as cooler, possibly with some increase in winter precipitation (Metcalfe et al. 2000).

Throughout the late Pleistocene, these sediment core studies show teleconnections to the North Atlantic. Both Henrich events and D/O events have been detected in various

regions throughout the tropics. During this time period Metcalfe et al. (2000) and Bradbury (1989) have found conflicting results for the conditions in Mexico and ~14 000 ka. Metcalfe et al (2000) recorded generally dry conditions, while Bradbury (1989) noted a moist terminal Pleistocene.

Early Holocene:

There are few records available from the Caribbean region that cover the early Holocene. A 7.7m sediment core from Lake Miragoâne, Haiti, is a notable exception, and spans the last 10300 ^{14}C yr BP (11960 cal yr BP). This record was developed using multiple proxies, including pollen, charcoal and stable oxygen isotopes from ostracods ($\delta^{18}O$) (Hodell et al. 1991). This study suggest that during the early Holocene and the latter part of the Younger Dryas, the climate was dry in this area, resulting in lower lake levels during this time (Hodell et al. 1991). The $^{18}O/^{16}O$ ratio recorded a general decreasing trend following the Younger Dryas and between ~10-7 kyr BP (Hodell et al. 1991). During this time period the lake level rose due to eustatic sea level rise, and wetter conditions persisted for ~4000 years. This transition was not linear between dry and wet, as two minima in the data were found at ~9.1 and 8.1 kyr BP (Hodell et al. 1991). This trend marks a switch from arid to humid conditions, which was documented throughout much of the tropics near the Pleistocene/Holocene boundary (e.g. Hodell et al. 1991).

Middle Holocene:

During the Middle Holocene Lachniet (2004) infers the presence of a tropical-extra tropical teleconnection to the 8.2 yr BP cold event. This was recorded from a stalagmite from Costa Rica that was dated between 8840 and 4920 yr BP using uranium/thorium (U/Th) techniques. The $\delta^{18}O$ values record an early Holocene dry

period correlative with the high latitude 8.2 yr BP cold event based on the high values found in the $^{18}O/^{16}O$ ratio between 8300 and 8000 yr BP. Supporting this study, Hodell et al. (1991) suggested that at Lake Mirâgoane, Haiti, the ratio of evaporation to precipitation was still high between ~10 and 8.4 kyr BP, as indicated by relatively high $\delta^{18}O$ values. Pollen assemblages for this lake, also indicate wide-spread dry conditions until ~8.2 kyr BP. The $\delta^{18}O$ values dropped between ~7 and 5.3 kyr BP coinciding with higher lake levels (Hodell et al., 1991).

In another study, Banner et al. (1994) identified a wet period through strontium isotope analysis from speleothems in Barbados. This proxy works on the principle that lower $^{87}Sr/^{86}Sr$ ratios occur during periods of higher recharge while higher ratios occur when recharge is diminished. During a period between 6-4 ka the Sr ratio indicates a period of maximum recharge, indicating a wet mid-Holocene, in conjunction with Hodell et al. (1991).

Moreover, van Hengstum et al. (2018) extracted five sediment cores from No Man's Land (NML), one of the largest in diameter inland lakes in the northern Bahamas, shows a transition at ~6500 cal yr BP from terrestrial peat deposition to carbonate mud with freshwater invertebrates and charophytes indicates the onset of aquatic conditions in NML (van Hengstum et al. 2018). Comparing this onset of aquatic conditions ~6500 years ago to the work of Hodell et al. (1991, 1995) and Fensterer et al. (2013b), this increase in regional precipitation is likely due to a more northerly displaced ITCZ (van Hengstum et al. 2018). Aquatic freshwater environments in the area would have been promoted by a more northerly ITCZ during the middle Holocene (van Hengstum et al. 2018).

The increased moisture found in the Bahamas at this time also coincides with increased Ti flux to the Cariaco Basin (Haug 2001) and the depleted $\delta^{18}O$ values in a speleothem from western Cuba (Fensterer et al. 2013b) (van Hengstum et al. 2018). These proxies all indicate that ~7000 to ~5000 years ago was one of the wettest periods during the Holocene in the Caribbean (van Hengstum et al. 2018).

During the middle Holocene a variety of speleothem and sediment core analyses were completed throughout the Caribbean. Many of these studies noted results showing an early Holocene dry period that corresponds with high latitude 8.2 yr BP cold events. Additionally, a speleothem study from Barbados and a sediment core study from the Bahamas both follow this early Holocene dry period with findings that support a wet mid-Holocene beginning at ~6 ka.

Late Holocene:

At No Man's Land (NML's) ~3300 years ago, the stratigraphic and microfossil evidence collectively indicates that a shallow stratified basin with freshwater cap abruptly transitioned into an anoxic marine setting (van Hengstum et al. 2018). It is known that intense hurricane activity can also be a significant factor causing salinization of costal carbonate aquifers, but 3300 to 2500 cal yr BP coincides with a less active period of intense hurricane activity on the western tropical North Atlantic margin (van Hengstum et al. 2018). It is hypothesized that a decrease in regional rainfall, which was superimposed upon the long-term signal of relative sea-level rise, would explain the abrupt loss of a freshwater lens in NML from 3300 to 2500 cal year BP – which has been referred to as the 'Pan-Caribbean Dry Period' (van Hengstum et al. 2018).

Looking back at Lake Miragoâne, records show that, between 3.2-2.4 kyr BP, a two-step increase in the $\delta^{18}O$ values indicates a trend toward higher evaporation rates and lower lake levels (Hodell et al. 1991). At 2.4 kyr a sharp increase occurs, marking the beginning of a dry episode that lasted from ~2.4-1.5 kyr BP. In a study from the Yucatan Peninsula, Hodell et al. (1995) documented a period of aridity from ~1300-1100 cal yr BP. This sediment record indicates significant droughts during this time that have been linked with the collapse of the Classic Maya civilization in Mesoamerica (Hodell et al. 1995). It has been estimated that the Terminal Classic Drought occurred between 770-1100 AD and included an early phase (770-870 AD) and a late phase (920-1100 AD). This 50-year period in between the dry phases was marked by more mesic conditions. These results are also consistent with findings from the Cariaco Basin, in the Caribbean Sea just offshore of northern Venezuela (Haug et al. 2003). This common occurrence suggests that the TCD was a wide spread phenomenon and not limited to the Yucatan region.

Later, Lane et al. 2011 used a high-resolution sediment core extracted from a small mid-elevation lake on the slope of the Cordillera Centra, Dominican Republic. In this record, positive isotope $\delta^{18}O$ values found between ~1300-1150 cal yr BP indicate aridity that correspond with other Caribbean records at this time. Another increase in $\delta^{18}O$ between 1000-650 cal yr BP is consistent with drought periods Haug et al. (2003) identified in the Cariaco Basin and may correspond to a "Late Phase" of the TCD (Lane et al. 2011). During this time period, it is hypothesized that a more northerly mean annual position of the ITCZ in the circum-Caribbean was in cause (Lane et al. 2011). This hypothesis roughly coincides with the interval recognized as the Medieval Climate

Anomaly (MCA). What is responsible for this shift is still unknown, but speleothem data from Scotland and tree ring data from Morocco suggest a positive phase of the North Atlantic Oscillation (NAO) may have played a role (Trouet et al. 2009) (Medina-Elizalde et al. 2010).

Further evidence of the TCD was found from two lakes in the Dominican Republic using multi proxies from multiple sediment cores (Lane et al. 2009). This found that increasing aridity was consistent with the TCD, although the results were discontinuous. Lane et al. (2014) used δD_{alkane} data, which complements the results from Lane et al. (2009), but also extends the record and confirms arid conditions coincident with the TCD. Lane et al. (2014) "believes that the impact of the TCD provided impetus from more subtle cultural transitions that included intensified agricultural practices and, paradoxically, population increases in the Caribbean."

In another study regarding the Maya terminal classic period, Medina-Elizalde et al. (2010) provides a potential explanation for the long 150-year socio-political decline of the Classic Maya Civilization. This reconstruction suggests that the drought prevailed during the Terminal Classic Period (TCP) and was likely an important factor in the disintegration of the Classic Maya civilization. Using the stable isotopes of oxygen from a speleothem, a direct calibration between the $\delta^{18}O$ and rainfall amount suggests that eight severe droughts occurred in the Yucatan Peninsula lowlands during the TCP. The droughts recorded represent rainfall reductions between 52 and 36%, and had durations of 3-18 years. It is hypothesized that these droughts triggered major depopulation events of the Maya kingdoms and city-states during the TCP. The intensity and short duration of

these droughts help explain why the TCP disintegration of the Maya civilization occurred over a 150-year period and not abruptly (Medina-Elizalde et al. 2010).

Another climate anomaly thought to be limited to the northern latitudes is the Little Ice Age (LIA). Increasing evidence reflects significant climate change in the tropics during this time period. Lane et al. (2014) hypothesized that the LIA has been identified in the Caribbean between 650 cal yr BP and the present. Their $\delta^{18}O$ record is very similar to the Cariaco Basin Ti concentration record (Haug et al. 2001) that suggest a more southerly mean annual position in the ITCZ, thereby producing more arid conditions through much of the northern tropics (Lane et al. 2011).

During the late Holocene, studies in the Caribbean have showed that drier conditions prevailed throughout this period in the Bahamas. van Hengstrum et al (2018) recorded a dry period between 330-2500 cal yr BP. This si supported by Hodell et al (1991) recording drying episodes between ~2.4-1.5 kyr BP. Lastly, Lane et al (2011) studied a sediment core from the Dominican Republic and found that between 1300-1150 arid conditions were present. These finding of aridity in the late Holocene correspond with many Caribbean records at this time.

1.1.2 Paleoclimate reconstructions in Cuba

Sediment Core Studies

There are a limited number of paleoclimate reconstructions for Cuba. The longest paleoenvironmental record for the island is from a 3 m long-sediment core record extracted from Laguna de la Leche (Peros et al. 2007). This multiproxy study used loss

on ignition (LOI), calcareous microfossils, pollen, and plant macrofossils. Where Laguna de la Leche is situated today appears to have been dry prior to ~6500 cal yr BP. By 6200 cal yr BP water started to fill the basin and a shallow lake formed. What caused this to occur was likely a rise in relative sea level (RSL), increasing the phreatic aquifer (Peros et al. 2007). The oxygen and strontium isotope data suggest that this oligohaline lake was almost permanently isolated from the sea due to isotopic values showing that this system was high in evaporation but low salinity. The water level was found to increase after ~4200 cal yr BP due to rising seawater using oxygen and strontium isotopic values that suggest a trend to more marine values.

In a study from a lagoon in southeastern Cuba, Peros et al. (2015) used a sediment core to investigate response to sea level change, climate change and to infer changes in the frequency of past hurricane strikes. This study used benthic foraminifera, fossil pollen, particle size analysis and macro charcoal influx values. During the period from 4000-2800 cal yr BP the area was flooded by rising sea levels where higher salinity values inferred from foraminiferal data were consistent with seawater intrusion.

Between 2800-2000 cal yr BP a freshening of the system occurred. The presence of large amounts of ostracods and a lack of foraminifera support the presence of a fresh or low-salinity environment. This freshening suggests a wetter period. From 2000-1000 cal yr BP salinities and water depth fluctuated, this is seen from the relatively diverse foraminiferal assemblages found indicating numerous sub-environments that would support a range of species (Peros et al. 2015). Finally, from 1000 cal yr BP to present, this time period may be associated with a second period of freshening, found from a

decrease in *Quinqueloculina* species, a decrease in foraminiferal diversity and an increase in *Ammonia tepida* (Peros et al. 2015).

Gregory et al. (2015) used a combination of foraminifera and X-Ray Fluorescence (XRF) elemental data from cores taken from two lagoons on the southwest coast of Cuba: Punta des Cartas and Playa Bailen. Foraminifera data from both cores show similar patterns of salinity shifts during the late Holocene, both locations show trends toward relatively more marine conditions spanning the last ~3000 yr BP similar in timing in assemblage transitions suggesting a regional vs. basin specific effect (Gregory et al. 2015). Moreover, the XRF elemental data show a clear increase in salinity and decrease in erosional inputs (inferred as a decrease in precipitation from elements Ti, Fe, K, Ti/Ca) at ~1400-1200 yr BP resulting in the onset of more arid conditions. Temporal correlation of other Caribbean paleoclimate records, suggest that trends observed at these two lakes were controlled by regional climate, likely associated with shifts in the position of the ITCZ (Gregory et al. 2015).

A multistage 8.2 kyr was detected using a sediment core from a sinkhole in Eastern Cuba (Peros et al. 2017). The 8.2 kyr event at Cenote Jennifer is characterized by abrupt changes in the Cl and Br count from XRF scans. These changes are found between ~ 8120 and ~8275 cal yr BP. that closely match the 8.2 kyr event identified in the NGRIP $\delta^{18}O$ record from Greenland. The increase in these elements represent a shift to drier conditions, which caused increased evaporation and the concentration of Cl and Br in the water at the base of the sinkhole. To support these increases, it was found that a lack of response in Fe and a minor response in Ti during the 8.2kyr event at Cenote Jennifer

supports the notion of a concentration of Cl and Br was due to higher evaporation, rather than an increase in sea level (Peros et al. 2017).

Speleothem Studies

In a 2001 study by Pajon et al. a speleothem from the Dos Anas cave system was examined and was shown to record abrupt climate warming at the end of the Pleistocene (~12 500 cal yr BP) using the $\delta\ ^{18}O$ stable isotope analysis of 9 samples from the stalagmite. The overall results from the analysis show increasingly negative values, possibly indicating a warming trend to the present. An abrupt warming was detected before the beginning of the Holocene, which was dated by ^{14}C to 11 520 +/- 50 years BP. This warming, which seems to have occurred during the Younger Dryas chronozone, may have been an unusual response to this climate event.

In a more recent speleothem study from Cuba, (Fensterer et al. 2013b) developed a high-resolution oxygen isotope record from two stalagmites from north-western Cuba. Like the other studies, stalagmite Cuba Peqceño was collected in the Dos Anas cave system, while stalagmite Cuba Medio was collected in the Santo Tomas Cave System. The proxy data from this study cover precipitation changes for most of the last 12 ka. This record shows a transition from higher $\delta^{18}O$ to more negative values between 10 and 6 ka. Additionally, a short peak of relatively high values was noted around 8.3 ka, reflecting drier conditions, which Fensterer et al. (2013) hypothesized may be related to the 8.2 kyr event. This shift toward more negative values is of relatively low magnitude in both speleothems, thus detailed insight into the 8.2 kyr event in the northern Caribbean was not possible in this study.

A study by Fensterer et al. (2012) represents the first high-resolution $\delta^{18}O$ record of a stalagmite from western Cuba. The 720 mm long stalagmite was also collected from the Dos Anas cave system. This record covers the Little Ice Age and Medieval Climate Anomaly with the $\delta^{18}O$ values suggesting drier conditions around 0.35 ka in the middle of the LIA and wet conditions during the MCA between 0.9-1ka. This record also indicates dry conditions during the Maya terminal classic period that are in agreement with results from previous studies (Medina-Elizalde et al. 2010;Lane et al. 2014). The $\delta^{18}O$ record of the stalagmite reflects precipitation variability in Cuba during the last 1.3ka. This can be interpreted in this manner because oxygen isotope measurements from speleothems have been used to infer past hydrological cycles because the isotopic composition of precipitation is observed to decrease with increasing precipitation rates over low latitude costal and island stations (Lee and Swann 2010). Owing to the amount effect, more rainfall on the island of Cuba leads to lower $\delta^{18}O$ values, therefore lower $\delta^{18}O$ values in speleothem calcite reflect wetter conditions (Fensterer et al. 2012).

Dating back to the Pleistocene, Warken et al (2019) extends previous paleoclimate evidence for Cuba back to 96 ka. Although, not continuous as this record shows a hiatus between ~93-81 ka. This study combined stable isotopes of oxygen and carbon with a trace element analysis. In this study, Warken et al (2019) found that North Atlantic cold events were recorded in the Caribbean. Henrich stadials, in particular, were associated with relatively cold and dry conditions in Cuba. This record showed that HS 1 was the driest and coolest interval of the whole record. During Greenland warm interstadials it was found that these produced relatively warm and wet conditions – especially during MIS 5. During the transition into the Holocene, the record shows a

gradual change to generally warmer and wetter conditions. This study is in agreement with Fensterer 2012 showing North Atlantic cold events that coincide with drier conditions in Cuba.

Overall, the records from Cuba are generally reflecting a shift to drier conditions from the middle to late Holocene. Many different proxy datasets, based on stalagmites and sediment cores, from different areas of the island, are beginning to help to develop a better understanding of the causes of Holocene climate variability in the Caribbean region. For example, many studies have suggested a southward shift of the ITCZ as a forcing mechanism for the low level precipitation during the late Holocene; this is fitting, as the ITCZ is one of the main drivers of precipitation on the island regularly.

1.1.3 Speleothems in Paleoclimate reconstructions

Speleothems have emerged as one of the most valuable resources for understanding Earth's surface conditions in the past (Fairchild et al. 2012). Speleothems are secondary mineral deposits, chemically precipitated in caves, principally from carbonate seepage waters (Agosta, 2010). These carbonate seepage waters are typically formed in karst landscapes. These landscapes can be defined by the distinctive hydrologic and geomorphic characteristics that arise from the unique combination of highly soluble rock with sufficient secondary porosity, in the case of this study – carbonate bedrock (Ford and Williams, 1989). The landforms and hydrologic patterns arise when portions of bedrock dissolve, and one of the most common features of such landscapes is the ubiquitous presence of subterranean conduits for water and material transport including

humanly traversable cave systems (Palmer, 2007). It is within these cave systems, where the conditions are relatively stable that speleothems are able to develop.

The process of speleothem deposition begins with rainwater seeping through these karst landscapes (Figure 1). In order for a speleothem to develop, the presence of calcium carbonate ($CaCO_3$) is needed in the host rock, as well as a sufficient water and carbon dioxide (CO_2) supply. The three main reactions involved in speleothem deposition can be found in the following set of equations:

$$H_2O + CO_2 \rightarrow H_2CO_3 \textit{ (carbonic acid)} \quad [1]$$

$$CaCO_3 + H_2CO_3 \rightarrow Ca^{+} + 2HCO_3 \textit{ (calcium bicarbonate dissolution)} \quad [2]$$

$$Ca^{2+} + 2HCO_3 \textit{ (aq)} \rightarrow CO_{2\,(g)} + H_2O_{\,(l)} + CaCO_{3\,(s)} \textit{ (calcite)} \quad [3]$$

Due to respiration and the decomposition of organic matter, a high carbon dioxide partial pressure (P_{CO2}) arises in the soil (Fairchild *et al.* 2012). As water percolates through the soil column above the calcium carbonate bedrock, additional CO_2 is absorbed due to the fact that the partial pressure of the soil CO_2 is much higher than atmospheric CO_2 (Fairchild *et al.* 2012). When the soil CO_2 mixes with water, the result is the formation of carbonic acid (Equation 1). When this percolating water, which has a high $P_{CO2,}$ reaches the calcium carbonate bedrock, the carbonic acid reacts with the $CaCO_3$ producing a calcium bicarbonate solution (Equation 2) (Fairchild *et al.* 2012). This reaction keeps occurring until the solution is saturated with calcium ions from the bedrock (Ca^{2+}). The final stage of speleothem deposition occurs when the water that is saturated with calcium reaches the cave's atmosphere. Since the P_{CO2} in the cave is lower than that of the water from the soil zone, the CO_2 is degassed from the solution (Fairchild et al. 2012). This degassing reduces the ability for the solution to hold the dissolved $CaCO_3$, and the

solution then becomes supersaturated with respect to calcite. This process of super saturation causes the reaction to reverse (Equation 3), and the carbonate minerals are then precipitated out of the solution, forming a variety of speleothem deposits in the cave environment (Agosta, 2010). The predominant mineral that precipitates in cave systems is calcite; however, aragonite and gypsum can also be found in speleothems (Fensterer, 2011).

Strong colour banding (yellow, brown, or red-brown) is commonly observed in speleothems and this colour inclusion can be due to the incorporation of organic compounds from soil waters above the cave (Van Beynen et al. 2001). Another possible source of colour are metals incorporated into the solution but these rarely provide visible colour (White, 2007). The annual banding seen in speleothems is similar to that of tree rings with alternating light and dark lamina. Light bands are inclusion rich and generally deposited during the season where rainfall is most abundant. What gives the bands the light colour is the high leaf litter production due to increased rainfall and a surge of fulvic acids in the soil, which are lighter in colour (White, 2007). The darker bands are due to the dryer-seasons, resulting from the extraction of darker humic aids from the soil (White 2007). These alternating light and dark lamina produce a highly resolved record of the environmental and climatic conditions during the time of deposition. Although, not all speleothems are represented by a continuous record of depositional growth, hiatuses can create discontinuities in the depositional record caused by drought, cold or change in groundwater routing (Frappier et al. 2007).

Finally, in order to interpret these paleoclimate proxies, the isotopes in the calcite crystals must be deposited in thermodynamic equilibrium with their parent drip waters at

slow degassing rates to ensure that the distribution of light and heavy isotopes between the aqueous and solid phase is only a function of temperature (Hendy, 1971 and Laurizten & Lundberg 1999). On the other hand, kinetic fractionation represents disequilibrium conditions which result in pronounced variations in observed $\delta^{18}O$ and $\delta^{13}C$ values. The consequence of this is an obscured climate signal due to the calcite not being in isotopic equilibrium with the drip waters (Lachniet 2009). Common causes of this disequilibrium are rapid crystallization, degassing in the epikarst and evaporation in the cave.

The Hendy Test is used to check for equilibrium deposition in speleothems, and is done by verifying an absence of covariance of the isotopes along a single lamina (Dorale 2009). This test is based on the premise that kinetic effects would lead to progressive enrichment in the isotopes as drip waters move over the stalagmite surface from the point of impact of the drip. When deposition occurs under equilibrium conditions, $\delta^{13}C$ becomes enriched as the drip moves from the apex to the sides of the stalagmite due to a limited amount of bicarbonate, where the $\delta^{18}O$ should not vary due to the relatively large amount of water available (Laurizten & Lundberg, 1999). If evaporation occurred, a significant amount of water will be lost along the same trajectory so that both heavy isotopes then become simultaneously enriched, owing to kinetic effects as the heavier ^{13}C and ^{18}O molecules are preferentially fractionated (Agosta 2010).

When analyzing stable isotopes from speleothems, a co-linear relationship between $\delta^{18}O$ and $\delta^{13}C$ should be viewed with suspicion as these variations in the data are likely attributable to kinetic isotopic fractionations and should not be used as geochemical proxies in paleoclimate research (Agosta 2010). However, covariance of

these isotopes with increasing $\delta^{18}O$ could have some paleoclimate value, as it can be indicative of significant drying and more evaporative conditions in the cave at the time of deposition.

Although the Hendy Test has been reported in many studies, the test itself has some limitations due to the difficulty of execution. These limitations include the challenges associated with sampling along a single growth layer, which can be difficult due to limited sampling precision, speleothem geometry, and variability in lamina thickness. Dorale & Liu (2009) also argue that several other limitations exist within the Hendy Test criteria for judging the paleoclimate suitability of speleothems. A discrepancy that Dorale & Liu (2009) mention is that isotopic equilibrium may occur in the center of the speleothem at the same time as kinetic fractionations occurs at the flanks. In addition, the criterion that there is no relationship between $\delta^{18}O$ and $\delta^{13}C$ along a growth band is based on the assumption that speleothem $\delta^{13}C$ values are not linked to climate, which is not necessarily true. Due to the fact that climate is directly related to soil biological productivity and vegetation type, in some cases a coupling of $\delta^{13}C$ and $\delta^{18}O$ values may not be related to kinetic isotope effects, but instead an indication of climate change. Dorale & Liu, (2009) advocate the need for replication of similar isotopic profiles between two or more stalagmites; however this too presents limitations, predominately with respect to cost restrictions and cave conservation.

1.2 Research objectives

In general, the records that have been studied in the Caribbean are low resolution and typically only cover the latest Pleistocene and Holocene. Thus, additional records are needed that have longer time-depth, and have high temporal resolution. Analyzing the

oxygen and carbon stable isotopes of a stalagmite from western Cuba will help fill these data gaps, and provide a more in depth explanation for northern Atlantic events and their effects in the Caribbean.

Using speleothems as proxies for paleoclimate research allows for insight into past climate change that other proxies are not able to provide. Due to the fact that speleothem archives are able to record continuous episodes of growth, that are thousands of years in duration, they can preserve information on timescales from days to hundreds of thousands of years (Farichild et al. 2012). Ice cores often have similar temporal resolution, but other archives tend to have strengths either in their high-resolution nature (e.g. tree rings) or long duration (e.g. deep marine sediments) (Farichild et al. 2012). Speleothems also provide excellent chronologies by virtue of their ability to be U-series dated, (Farichild et al. 2012). Lastly, speleothems are both physically and chemically robust and are relatively well protected from erosion and other post-depositional processes. (Farichild et al. 2012).

Although, like any proxy archive, speleothems do have limitations. For example, sometimes interpretations are unduly speculative or too simplistic in terms of attributing a climatic explanation to the change in the speleothem record, as factors other than climate (such as vegetation), can be important at determining speleothem chemistry (Farichild et al. 2012). In addition, some speleothems can contain hiatuses, which can relate to dry periods in the cave environment, or other processes. After analyzing both the strengths and weakness of speleothem studies one of the major steps that need to be taken in this field is a more sophisticated understanding of how speleothem records contribute to understanding climate drivers and tele-connections of climate (Farichild et al. 2012). As

well, continued development of new types of proxy and the more effective use of multiproxy approaches need to be considered (Farichild et al. 2012).

This thesis will use a stalagmite to develop a long-term record of precipitation from the Pinar del Rio Province in Cuba. In completing this, these results will contribute new data to help our understanding of precipitation variability over the late Pleistocene. The specific questions that this thesis will address are:

1. Can this stalagmite be used for paleoclimate reconstruction?
2. Which known Pleistocene climate events can be identified through geochemical analysis of the speleothem?
3. Are other climatic changes, such as precipitation variability and droughts recorded in the Western Cuba region?

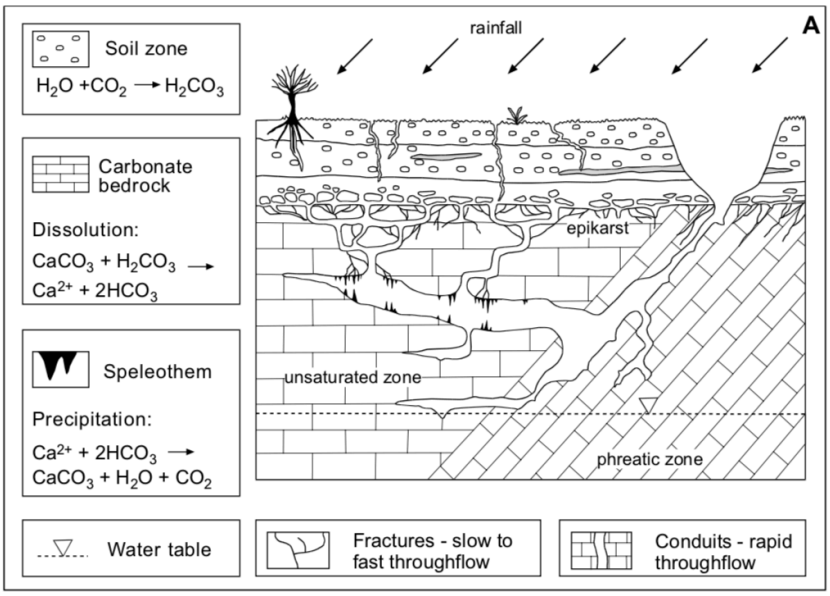

Figure 1: A simplified model for the deposition of calcite speleothems (Fairchild *et al*., 2006)

Chapter 2 - Pleistocene precipitation changes using O and C isotopes on a speleothem from the Majuanas Cave System, Cuba

2.1. Introduction

The study of climate change through the Pleistocene to the present can contribute to a better understanding of the magnitude and rates of change of natural climate variability in the context of current global warming. Few paleoclimate records in the Caribbean extend into the last glacial period mostly due to the lack of preservation or availability of suitable, high-resolution climate proxies (van Beynen *et al.* 2017).

Pajón et al. (2001) collected a speleothem from the Dos Anas cave system in the Province of Pinar del Rio, western Cuba. This stalagmite recorded abrupt climate warming at the end of the Pleistocene (~12500 cal yr BP) using the $\delta^{18}O$ stable isotope analysis of 9 samples from the stalagmite. This abrupt warming may be an unusual response associated with the Younger Dryas climate event (Pajón et al. 2001). Fensterer et al. (2013) developed a high-resolution oxygen isotope record from two stalagmites from the same cave system, which provided a nearly continuous, high-resolution $\delta^{18}O$ record of past precipitation changes during the last 12 ka. The record from these speleothems included major climatic anomalies, such as the Younger Dryas (12900-11700 cal yr BP) and the 8200 cal yr BP (8.2 ka) event (Fensterer et al. 2013). The speleothem record produced by Fensterer et al. (2013) suggests a general relationship between North Atlantic climate and precipitation in the northern Caribbean during the Holocene. This relationship was determined by the detection of Bond events in the speleothem record.

The longest paleoenvironmental record for Cuba comes from 3m long-sediment core

extracted from Laguna de la Leche by Peros et al. (2007a). A multi-proxy analysis of paleosalinity was further undertaken at the same locale by Peros et al. (2007b). This study allowed for the determination of the degree of connectivity that Laguna de le Leche has with the sea and how this has changed with time, the causes of these changes, and the effects of these changes on the salinity and water depth of the wetland (Peros *et al.* 2007).

Furthermore, Gregory et al. (2015) used a combination of foraminifera and X-Ray Fluorescence (XRF) elemental data from cores taken from two lagoons on the southwest coast of Cuba: Punta des Cartas and Playa Bailen. Sediment Ti concentrations, used to infer the amount of terrigenous input into an aquatic system, are high at 4000 yr BP and progressively decrease, with a distinctive decline recorded in both records at 1200–1100 yr BP, indicating drier conditions and less freshwater entering the lagoons at this point (Gregory et al. 2015). Similarly, a speleothem studied by Fensterer et al. (2012) from the Dos Anas cave system was based upon high-resolution $\delta^{18}O$ values over the last 1300 years. The speleothem record was strongly correlated to the Atlantic Multidecadal Oscillation for the last 1300 yr BP and recorded dry conditions during cold phases in the North Atlantic (such as the LIA), suggesting teleconnections between the northern Caribbean and the North Atlantic climate during the late Holocene (Fensterer et al. 2012).

Overall, the records from Cuba are generally reflecting a shift to drier conditions from the middle to late Holocene. Many different proxy datasets, based on stalagmites and sediment cores, from different areas of the island, are beginning to help to develop a better understanding of the causes of Holocene climate variability in the Caribbean region.

In general, the records that have been studied in the Caribbean are low resolution and typically only cover the latest Pleistocene and Holocene. Thus, additional records are needed that have longer time-depth, and have high temporal resolution. Analyzing the oxygen and carbon stable isotopes of a stalagmite from western Cuba will help fill these data gaps, and provide a more in depth explanation for northern Atlantic events and their effects in the Caribbean. The objective of this study is to develop a long-term record of precipitation from the Pinar del Rio Province in Cuba. In doing so, these results will contribute new data to help our understanding of precipitation variability over the late Pleistocene.

2.2 Regional setting

Stalagmite Majaguas Cave (MCS-01) was collected in the "Salon de la Permencia" (bedroom hall) of the Majaguas Cave, which is part of the Majaguas-Cantera Cave System (22° 23' N, 83° 58' W) (Figure 2). The Majagus-Canteras Cave system is found in Pinar del Rio Province, which is located on the western side of the island. Pinar del Rio Province contains one of Cuba's main mountain ranges - the Cordillera de Guaniguanico. This mountain range is divided into the Eastern Sierra del Rosario and the Western Sierra de Los Organos. The Majaguas-Cantera Cave system lies in the karst of the Sierra de San Carlos, which are part of the Sierra de los Organos mountain range (Figure 3). The Cave system has a total length of 35 km of galleries and has 10 levels of caverns and owes its origin to erosion and dissolution processes driven by external drainage, which crosses the massif from south to north and by the internal drainage system of the massif itself (Pajon et al. 2006). MCS-01 grew at 110m above sea level and

200m below the surface (Figure 4). The cave is covered by thick forest and soil. The sampling location belongs to the Salon de la Pemanencia and is located 300m from the cave entrance.

Pinar del Rio Province has a moderate subtropical climate with two seasons: the dry season from November to April and the humid season from May to October. Pinar del Rio is classified as "Am or tropical monsoon climate" according to the Koppen-Geiger climate classification, with the average annual temperature being 24.9 degrees Celsius and the average rainfall accumulation is 1353 cm.

2.3 Materials and methods

The MCS-01 sample was cut down its central growth axis using a Target tilematic 14" diamond blade with continuous rim and polished to show the internal details of the stalagmite (Figure 5). Following this, calcite samples (~1g) were taken from one half of the speleothem along visible growth layers and hiatuses using a hand held Dremel Rotary tool with a 0.3 mm diamond tip drill bit for U-Th radiometric dating. The positions of the samples was based on their proximity to hiatuses that were observed in the interior of the stalagmite, and an attempt was made to sample calcite as close as possible to these hiatuses.

Samples for stable isotope analysis (oxygen and carbon) were taken from the same half of the stalagmite using the hand-held Dremel Rotary tool fitted into a Dremel Rotary Tool Workstation Drill Press. The sample was placed on a velmex tree ring counter, in order to accurately sample the speleothem at 1mm intervals along the growth

axis, where ~700-800 µg of sample was collected (Figure 6). Stable isotope samples were processed at the University of Ottawa's Ján Veizer Stable Isotope Laboratory.

2.3.1 ^{234}U-^{230}Th Chronology

The U-series measurements for age determination were performed at the Radiochronology laboratory of the GEOTOP-UQAM-McGill Research Center, Quebec, Canada. Each 1g of subsample powder was dissolved using nitric acid in a Teflon™ beaker into which a weighed amount of calibrated mixed spike ^{233}U-^{236}U^{229}Th had been placed and evaporated slowly to dryness. After the dissolution, around 10 mg of iron carrier was added and the solution was then left overnight for spike-sample equilibrium. U and Th were coprecipitated with $Fe(OH)_3$ by adding ammonium hydroxide drop by drop until reaching pH 8-9. The precipitate was recovered by centrifugation and washed twice with deionized water, then dissolved in 6 N HCl. U-Th separation was performed on a 2 mL AG1X8 anionic resin volume. The thorium fraction was recovered through elution with 6 N HCl, and the U and Fe fraction, with water. The U fraction was purified on a 0.2 mL U-Teva™ (Elchrom industry™) resin volume. Fe was eluted with 3 N HNO_3 and the U fraction with 0.02 N HNO_3. After drying, thorium purification was carried out on a 2 mL AG1X8 resin in 7 N HNO_3 and eluted with 6 N HCl. U-Th measurements were performed using a multicollector inductively coupled plasma mass spectrometry Nu instrument™. ^{236}U-^{235}U-^{234}U-^{233}U and ^{232}Th-^{230}Th-^{229}Th were measured on the ion counter (IC0) in peak switching mode for uranium and thorium isotopes, respectively. ^{238}U was not measured by calculated from ^{235}U/^{236}U ratios, assuming a constant ^{238}U/^{2335}U mass ratio (137.88). Knowing ^{236}U/^{233}U of the spike, mass bias corrections in

atomic mass unit (amu^{-1}) were calculated and used to correct measured ratios between U isotopes and between Th isotopes (Ponte et al. 2017).

2.3.2 Stable isotope analysis

Oxygen isotope values (^{16}O and ^{18}O) and carbon isotope values (^{12}C and ^{13}C) were measured for 363 calcite samples drilled at discrete 1 mm intervals down the growth axis of the stalagmite. Approximately 500-700 µg of calcite was weighed for each sample and transferred to the exetainer for analysis. Stable isotopic analyses was conducted at the Ján Veizer Stable Isotope Laboratory, where 0.1 mL of degased anhydrous phosphoric acid was added to the exetainer, while on its side. Once all vials had acid added, the exetainers were flushed and filled with UHP helium off-line for 4 minutes at a rate of 60-70 mL/min. Following this, the vials were then immediately placed upright and in the heating block of the GasBench, and left to react for 24 hours. A regular analysis of the CO_2 headspace followed, using a Thermo Finnigan DeltaPlusXP IRMS. The isotopic composition of the $CO_{2\ (g)}$ for each sample was measured relative to the international reference, the Vienna Pee Dee Belemnite (VPDB), using the conventional "δ-per mil" notation. The analytical precision of this instrument is +/- 0.15‰.

2.4. Results

2.4.1 Description of stalagmite

The stalagmite measured 396mm in length along its growth axis. White calcite is visible in its interior (Figure 7). The growth axis is relatively straight, requiring only minor deviations along the path that the calcite samples were drilled. The presence of light brown lines parallel to the exterior perimeter of the stalagmite are interpreted as

weathering rinds and therefore hiatuses in the formation of the stalagmite. The first hiatus extends to approximately 100 mm from the end of the stalagmite, whereas the second hiatus almost corresponds to the exterior of the stalagmite. The presence of light brown inclusions are present after the first hiatus which may represent the incorporation of mud into the calcite matrix. The sections of the stalagmite after hiatus 1 and hiatus 2 also show numerous thin laminations which are absent in the older stalagmite section (before hiatus 1).

2.4.2 U/Th dating

Dating of MCS-01 produced ages on six of the seven samples submitted (Figure 8; Table 1). These results indicate that the stalagmite experienced three periods of growth: 100.545 ka - 68.222 ka (MIS 5c to MIS 4, late Pleistocene); 11.022 ka – 10.557 ka (early Holocene); and 0.409 ka – present (when the sample was collected) (late Holocene). The hiatus' between these time periods are distinct and clearly delineated, and therefore indicate that the stalagmite was inactive from approximately 68 – 11 ka and 10.5 – 0.4 ka.

In order to assign ages to each of the stable isotope measurements, three different age models were developed based on the data in Table 1. The earliest three dates were modeled using a second-order polynomial and show that speleothem growth between 100 - 68 ka was curvilinear and slowed with time. It is important to note, however, that there are only three dates over this 32,000 year period, and additional dating control could change this relationship. The second period of stalagmite growth occurred from ~11.0 – 10.5 ka and this has been modeled using a linear fit as only two dates are available.

Nevertheless, the short time span (approximately 500 years) of this interval suggests that the chronology of this section of the stalagmite is much more reliable than the earlier late Pleistocene section. Finally, the most recent period of stalagmite growth appears to have begun approximately 400 +/- 70 years ago. Assuming that the stalagmite was active when it was collected, as has been reported (Pajon, personal communication, 2017), the end of the stalagmite corresponds to the present. Therefore, a linear fit was used to assign ages to the stable isotopes in this section, and the chronology of this section is considered to be reliable, spanning a similar period of time (400-500 years) as the section dating to the early Holocene. Overall, stalagmite growth was considerably slower for the samples from the early and late Holocene compared to the late Pleistocene samples.

2.4.3 Stable isotope results

Results from this study show considerable variability between the growth periods (Holocene vs. Pleistocene) in the range of both the $\delta^{18}O$ and $\delta^{13}C$ values (Figure 9). During the Pleistocene period (green lines), $\delta^{18}O$ values ranged from -1.1‰ to -4.28‰ and the $\delta^{13}C$ values ranged from -2.4‰ to -11.88 ‰. $\delta^{18}O$ values are consistently low from 240-260 mm and then undergo an abrupt increase to near -1‰. The $\delta^{13}C$ values in this section of the stalagmite, however, respond in an inverse manner, becoming more negative and reaching values of approximately -10‰. Prior to this, $\delta^{18}O$ and $\delta^{13}C$ values show similar peaks and troughs, and are likely correlated. In the early Holocene section of the stalagmite (blue lines), $\delta^{18}O$ values range from -0.48‰ to -5.25‰ and -1.5‰ to -12.85‰ for $\delta^{13}C$. This time period has a much greater range and variability compared to the late Pleistocene, and both the $\delta^{18}O$ and $\delta^{13}C$ values show a consistent increase

throughout this period, before undergoing abrupt decreases. For the late Holocene section (red lines), the $\delta^{18}O$ and $\delta^{13}C$ values are the least variable; these values are -3.21‰ to -5.72‰ and -7.4‰ to -13.15 ‰ respectively and also show a general increasing trend toward more positive values.

2.5 Discussion and conclusions

2.5.1 Stalagmite formation and hiatuses during the late Pleistocene and Holocene

A recent synthesis of speleothem paleoclimatology for the Caribbean, Central America, and North America indicates that stalagmite MCS-01 represents one of the oldest (albeit non-continuous) speleothems from this region (Figure 10; Oster et al., 2019). Figure 10 shows a summary of speleothem growth periods and hiatuses with very few records spanning the period from 100 – 68 ka, with the exception of Devil's Hole, USA (Moseley et al., 2016), Leviathan Cave, Nevada (Lachinet et al., 2014), and Buckeye Creek, West Virginia (Springer et al., 2014). In the Caribbean, a recently published stalagmite record from the Santo Tomás cave system in western Cuba has yielded an almost 100,000 year-long stable isotope and elemental concentration (Ca, Mg, P, and U, Sr) record but shows a hiatus between ~93 – 81 ka (Warken et al., 2019), a timespan which is covered by stalagmite MCS-01. Thus, the MCS-01 record fills an important spatial and temporal gap in the speleothem record for North America, Central America, and the Caribbean.

2.5.2 Activity and inactivity of MCS-01 and possible causes

Not all speleothems are represented by a continuous record of depositional growth; hiatuses can create discontinuities in the growth record. Although it is known that the growth phases of stalagmites are usually indicative of wetter conditions (Oster et al., 2019), growth hiatuses do not necessarily invoke drier conditions. Growth hiatuses in stalagmites could be due to a variety of factors such as persistent dry conditions (Baker & Fairchild 2012), hydrological changes that cause the drip water to divert its path (Baker & Fairchild 2012), or a submergence of the cave due to sea level rise or flooding (Frappier et al. 2014). Sometimes, wetter conditions induce more vegetation cover and, therefore, depending on the cave, the surface water may not be able to infiltrate deep enough and make it to the drip site (Baker & Fairchild 2012). In order to reliably determine the cause of hiatuses, other proxy records need to be used to identify potential dry periods or other climatic perturbations that may cause the hiatus to occur. The most reliable way to determine the cause of a hiatus is through the analysis of a network of stalagmites from the cave and region to identify common climatic signals.

In the case of MCS-01, the cause(s) of the hiatus' can be narrowed down based on the geographical location of the stalagmite and information provided by other paleoclimatic studies. For example, sea level change and associated flooding of the cave can be ruled out as a cause due to the elevation of the speleothem, which grew at approximately 110m above sea level. However, MCS-01 also grew at a depth of 200m below the surface, which is covered by thick forest over think soil. This location is quite deep compared to stalagmites sampled near the surface. This could make MCS-01 more

sensitive to large scale changes in precipitation because of the difficulty water may have reaching this depth.

The initiation of MCS-01 corresponds to a relatively wet phase in the late Pleistocene (MIS-5c) based on a plot of the *G. ruber* foraminifera $\delta^{18}O$ record from the Caribbean Sea (Figure 11; Schmitt et al., 2006). Another observation is that the first hiatus (beginning at 68ka) corresponds closely to a drop in SST as inferred by the $\delta^{18}O$ record recorded in this marine core (Schmitt et al., 2006). Assuming that warmer SSTs in the Caribbean are associated with more precipitation (Oster el al. 2019), then the abrupt drop in SST/precipitation associated with the transition from MIS 5 to MIS 4 might have caused hiatus 1. Another important observation regarding MCS-01 is the reactivation around 11ka, when the climate in the Caribbean is starting to get warmer/wetter at the transition between MIS 2 and MIS 1. In short, the inactive period in MCS-01 between 68-11 ka corresponds closely to marine isotopes stages 4, 3, and 2, which are widely associated with cold and dry conditions, and this may explain the long hiatus in MCS-01.

The second hiatus in this record occurred from approximately 10500 ka to 400 ka (but possibly earlier). The cause of this growth hiatus is unknown, especially due to the proxy data from the Caribbean indicating that the early Holocene was a very humid period with ample precipitation (Haug et al., 2006; Hodell et al., 1991). Some hypotheses for this hiatus include the possibility of a local-scale hydrological change that caused the drip water to divert away from the site of the stalagmite or that the conditions were so wet during the Holocene that the cave actually flooded. However, due to the history of the climate in this area (Fensterer et al., 2013), it is more likely that the cause of this hiatus was a local scale hydrological change. Interestingly, MCS-01 appears to have been

active over the last 500 years, including during the LIA, which was probably the driest period of the Holocene in the Caribbean (Lozano-Garcia et al., 2007). In conclusion, overall the causes of the hiatuses are related to a combination of climatic and local-scale factors, but additional work will be needed to validate this.

2.5.3 Isotopic data

While the individual hiatuses in stalagmite MCS-01 are well dated, the limited number of dates between hiatuses means that the chronology of the $\delta^{18}O$ values must be considered provisional. That being said, all the dates are in chronological order, and they permit a preliminary comparison between the data in MCS-01 and other proxy datasets that allows for interpretation within a paleoclimate context. The focus of this discussion section is on the $\delta^{18}O$ data from MCS-01, which is interpreted as representing a primarily climatic signal, with more positive $\delta^{18}O$ values indicative of drier climate conditions, and more negative $\delta^{18}O$ values wetter conditions (Oster al., 2019; Fensterer et al., 2013; Warken et al., 2019). The carbon isotopic results from speleothems are more complicated and can be indicative of a number of other processes in addition to climate change, such as vegetation productivity (Fensterer et al. 2012); while these are generally correlated with the $\delta^{18}O$ data from MCS-01 (suggesting that they also record a climate signal; Figure 11), the remainder of the discussion deals mostly with the $\delta^{18}O$ data.

In terms of comparison to other local studies, Warken et al. (2019) has one of the few records from Cuba that dates to MIS 5 (based on stalagmite "Cuba Medio"), although it is mostly discontinuous though the time-period covered by MCS-01. The results of this study show the more negative (wetter) $\delta^{18}O$ values occur during MIS 5

(Warken et al., 2019), consistent with the data from MCS-01. This record also indicates relatively positive (dry) $\delta^{18}O$ values ranging from -1.5‰ to 0‰ during the last glacial period after the early MIS 4 (65ka) until 15ka BP. Though there are few other similarities between the record produced by Cuba Medio and the MCS-01 record, a few points of comparison do occur, such as that between 80-74 ka, and the termination of the MCS-01 record at 68 ka and where $\delta^{18}O$ isotope record from Warken et al. (2019) starts. At this time the $\delta^{18}O$ of MCS-01 sees values around -2‰, and one section of the Cuba Medio record also begins with values of -2‰ when MCS-01 enters a growth hiatus, indicating potential for these records to be considered as extensions of each other.

One of the main differences between the Cuba Medio and MCS-01 stalagmites, however, is the fact that the former is active after 68 ka whereas the latter is inactive (Figure 13). It is unclear why this is the case, as both stalagmites come from the same region of Cuba and therefore developed under a similar climatic regime. However, speleothem Cuba Medio was collected in Torch Cave (western Cuba) at 170m above sea level, which is overlain by approximately 60 m of rock. This is in contrast to the ~100 m of rock overlying stalagmite MCS-01, and it may be that Cuba Medio was active after 68ka because the overlying rock cover at the site of MCS-01 was thicker (and more densely vegetated), which meant that when conditions became drier during MIS 4, 3 and 2, it was just enough to limit water infiltration into the cavern where MCS-01 formed. Nevertheless, the similarities and differences between Cuba Medio and MCS-01 provide important information to help evaluate and interpret future late Pleistocene speleothem records from western Cuba.

The $\delta^{18}O$ results have also been compared to the NGRIP ice core (Figure 14) to analyze the MCS-01 data for evidence of a tropical response to high northern latitude climatic changes. A defining characteristic of the climate of the North Atlantic region during glacial times is the presence of both Dansgaard–Oeschger (D-O) events and Heinrich events (Warken et al. 2019). The former, D-O cycles, occurred approximately 25 times is a quasi-periodic nature and are characterized by a sudden onset of warm conditions followed by a gradual relaxation toward cool conditions following a period of approximately 1500 years (Greene et al. 2008). The latter, the Heinrich events, are associated with the delivery of large amount of "ice-rafted debris" (IRD) to the North Atlantic Ocean by icebergs which calved from the Laurentide Ice Sheet, as well as large amounts of freshwater which appears to have had important implications for influencing the Thermohaline Circulation (Little et al. 1997). One of these consequences is that the North Atlantic Ocean became colder, and the flux of icebergs indicates a degree of instability of the Laurentide Ice Sheet, although the causes of Heinrich events are not well understood (Marshall and Koutnik, 2006). Nevertheless, a few studies have shown that both D-O and Heinrich events drove changes in subtropical and tropical climate (Grimm et al., 2001), and the generation of new paleoclimatic data from tropical regions that has evidence of these events is important to help us better understand tropical-high latitude climate connections.

The $\delta^{18}O$ data in MCS-01 shows a pattern that is very similar to the D-O and Heinrich events clearly recorded in the NGRIP ice core, especially at ~82ka and between 78-70ka. This suggests that the stalagmite data are sensitive to high northern latitude climatic changes and indicates a possible teleconnection between the two regions. In

addition, the $\delta^{18}O$ data from MCS-01 also shows signs of relatively high-frequency periodicity in the data from MIS 5, which also suggests possible climate forcing. Because of small number of dates in this section, a spectral/wavelet analysis was not undertaken, but these fluctuations seem to occur with a periodicity of 1000-2000 years, which are broadly comparable to the D-O cycles seen in the NGRIP data. These relationships reflect the bipolar seesaw in which cold conditions in the North Atlantic are linked via the thermohaline circulation to warm conditions in the tropics, such that cold conditions in the North Atlantic are associated with a southward displacement of the Inter-Tropical Convergence Zone (ITCZ), and hence dry conditions in Cuba.

Table 1: Summary of dating results.

Sample Number	Depth range (mm)	Average sample point (mm)	Age (ka)	Error (ka)
MCS-1	0-13	6.5	100.545	2.55
MCS-2	274-288	281.0	68.222	1.803
MCS-3	291-303	297.0	11.022	0.25
MCS-4	359-369	364.0	10.557	0.257
MCS-5	371-377	374.0	0.409	0.07
MCS-6	380-389	384.5	No date	n/a
MCS-7	127-139	133	98.752	2.554

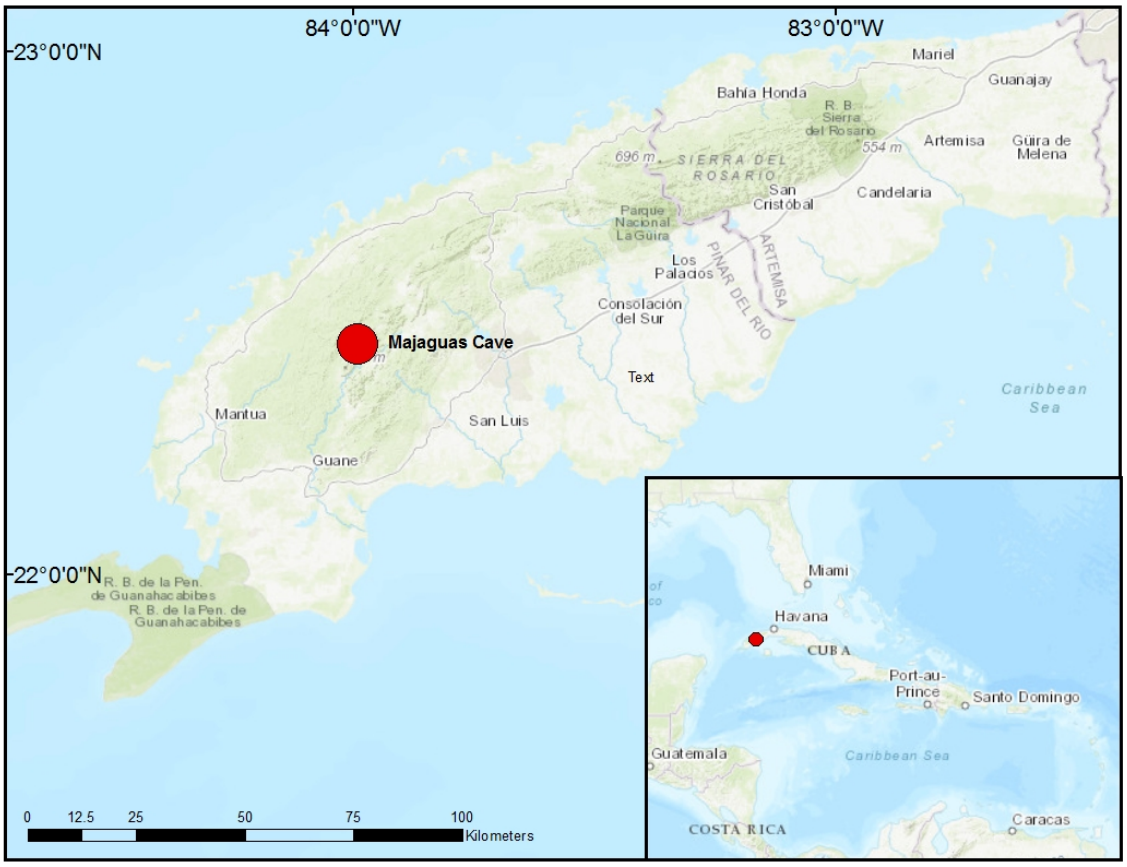

Figure 2: Location of the karst of Sierra de San Carlos and the Majaguas-Cantera Cave System in western Cuba, Pinar del Rio province, Cuba.

Figure 3: Karst of Sierra de San Carlos, Sierra de los Organos, Pinar del Rio province, Cuba (Photo: A. González).

Figure 4: Location of the stalagmite MCS-01 in the "Salón de la Permanencia", Majaguas Cave, Sierra de San Carlos, Cuba.

Figure 5: MCS-01 cut and polished to reveal internal structure.

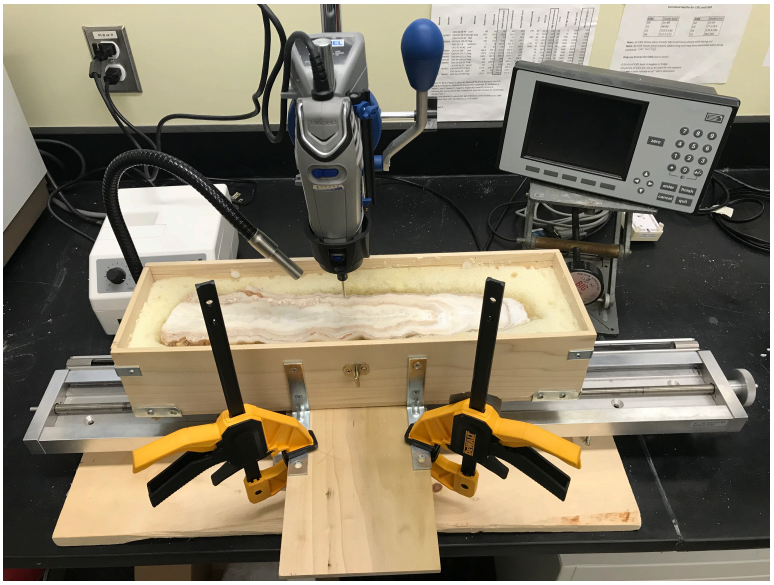

Figure 6: Sampling set up for stable isotopes.

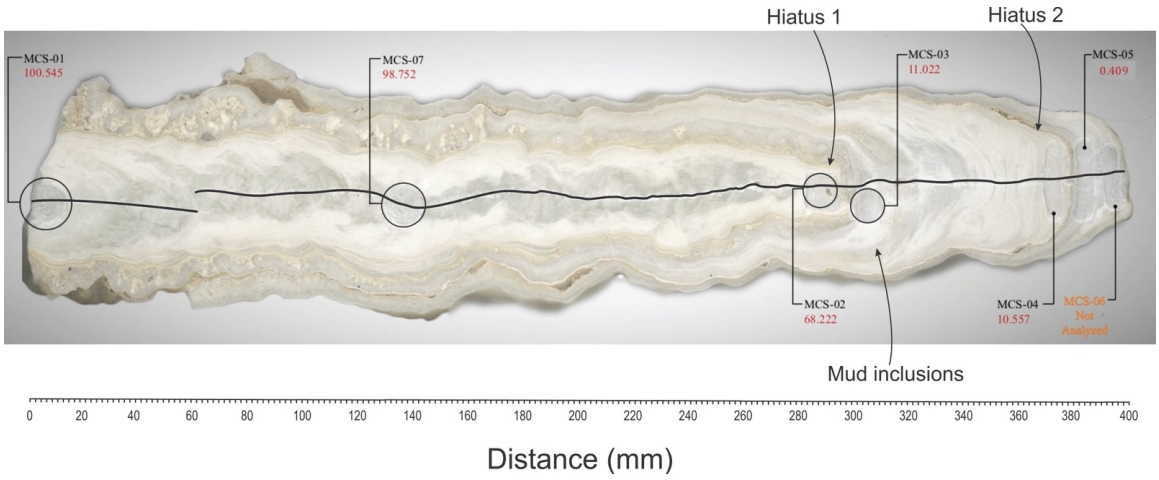

Figure 7: Stalagmite MCS-01 with base toward the left. Positions of U-Th dates are shown. The unsuccessful date is in orange. The positions of the two hiatuses and the mud inclusions are also labeled. The line along which samples were drilled for stable isotope analysis appears horizontally in the center of the stalagmite in black.

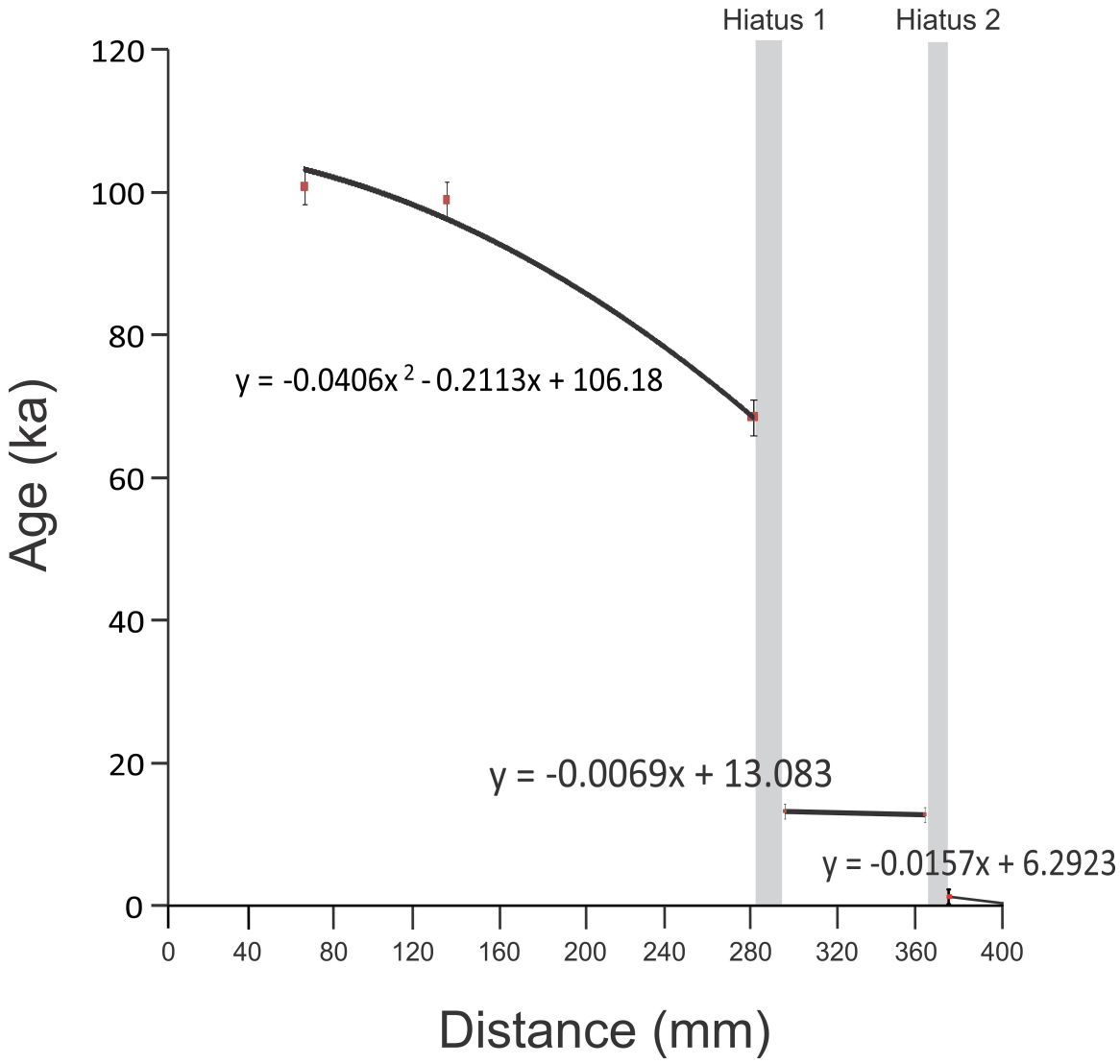

Figure 8: Age depth models for stalagmite MCS-01. The second-order polynomial that was used to fit the dates in the older section of the stalagmite lies within the error bars of each date from that section. In the other two cases, linear models were used because only two dates were available (including the tipoff the stalagmite, which was assumed to represent the present, in the case of the most recent age model.

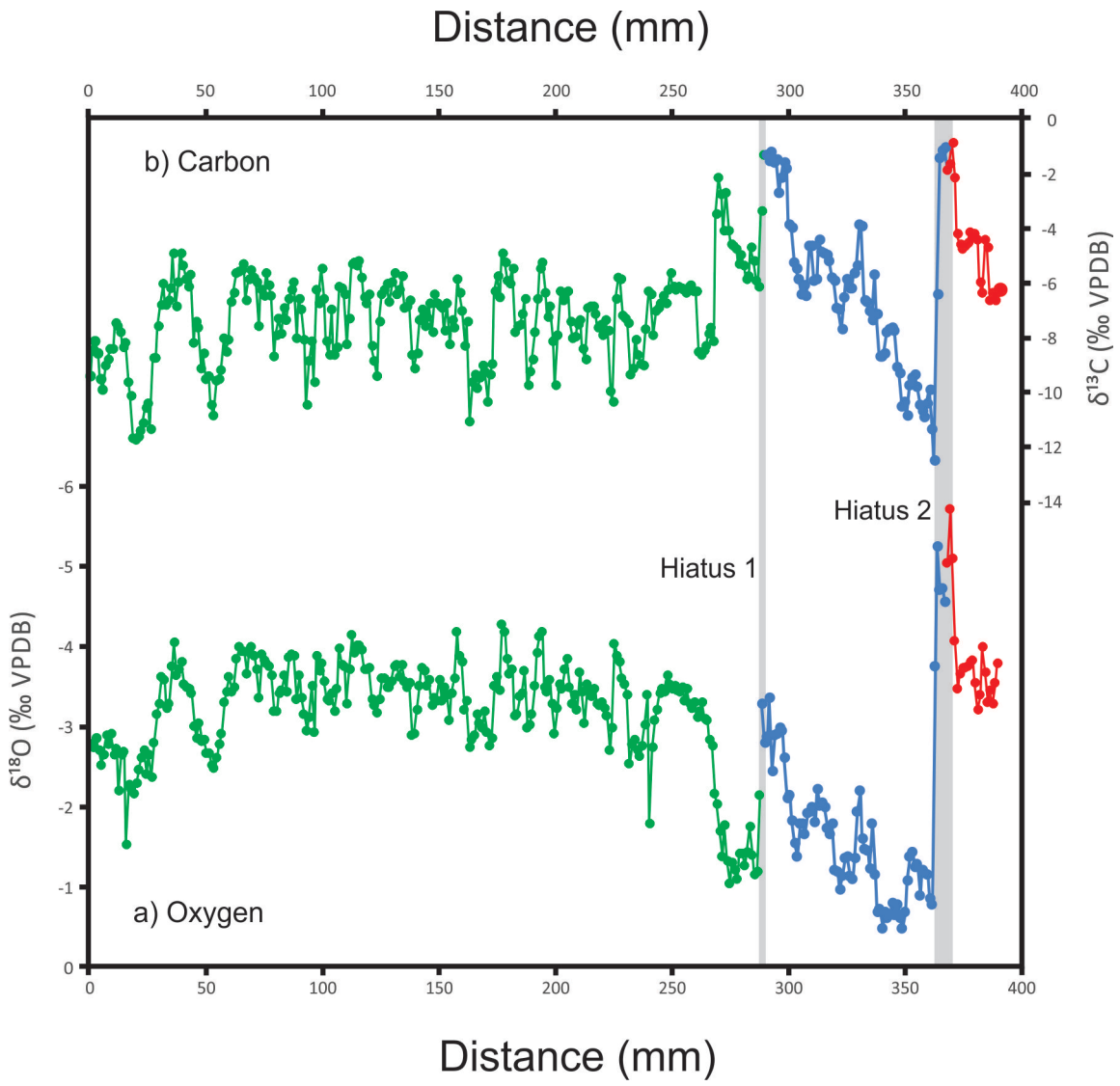

Figure 9: Results of the stable oxygen (a) and carbon (b) isotope analysis for stalagmite MCS-01. The boundaries between the green, blue, and red data are defined by the positions of the hiatuses.

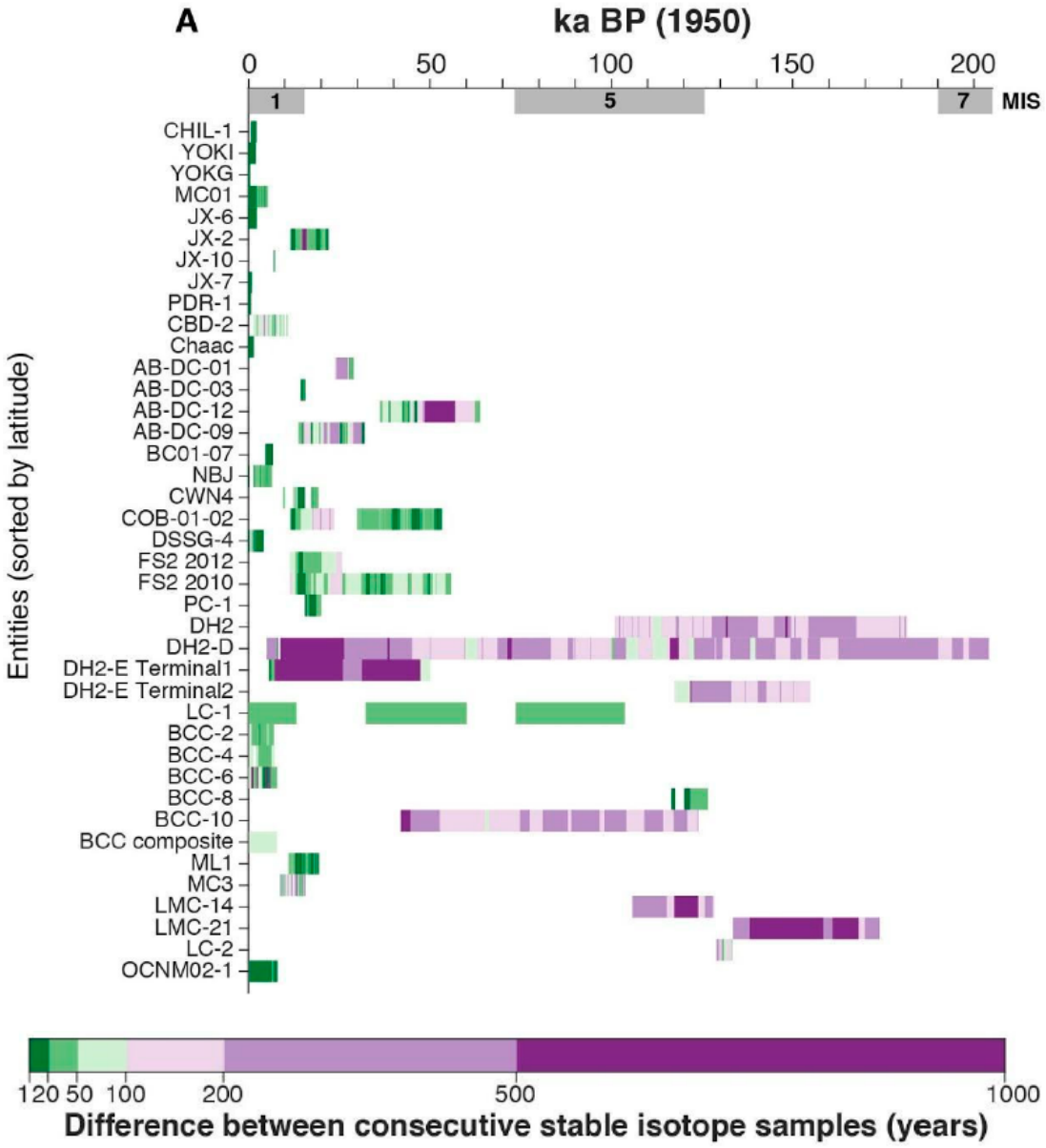

Figure 10: Temporal coverage of North and Central American and Caribbean speleothem records for the last 200 ka. The records are ordered by latitude along the y-axis (top is farther north). Coloured sections represent periods of active speleothem growth; the lack of colour represents hiatuses. The temporal resolution of the speleothem records is indicated by the colourd bands with darker green shading representing higher resolution.

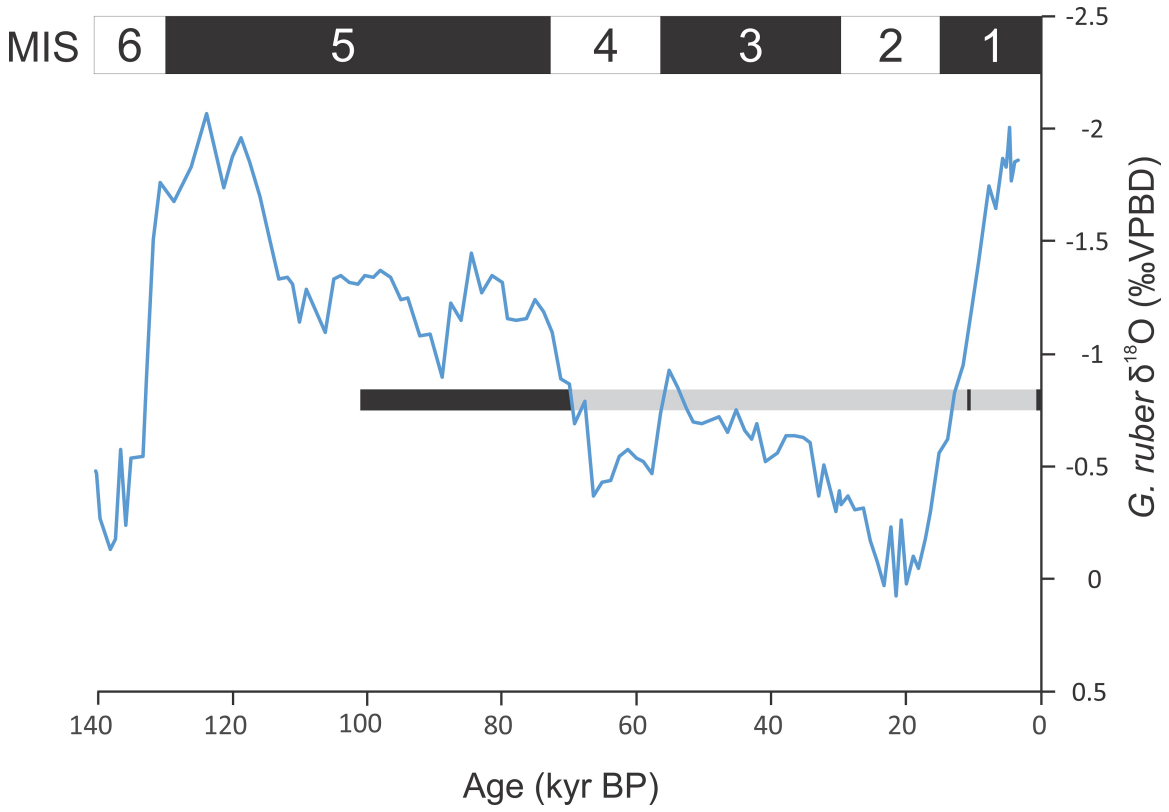

Figure 11: Active and inactive phases of stalagmite MCS-01 plotted alongside the *G. ruber* d18O record from the Caribbean Sea (indicative of sea surface temperature; reference). Active growth of MCS-01 is shown by the black horizontal bar; inactivity is shown by the grey horizontal sections. Marine isotopes stages 1-5 are plotted along the top of the chart.

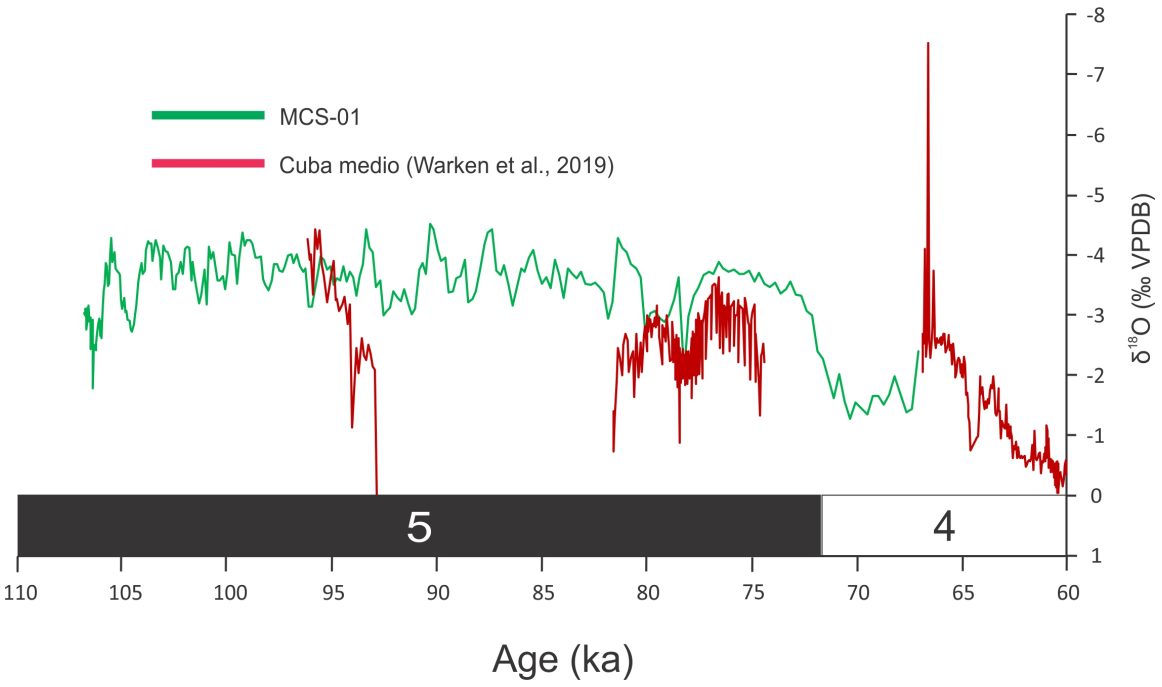

Figure 12: Oxygen isotope data from MCS-01 (green) plotted with the oxygen isotope record from stalagmite Cuba Medio (red; Warkern et al., 2019). The isotope data from Cuba medio is discontinuous between the period 100-66 ka. Marine isotopes stages are plotted at bottom of chart.

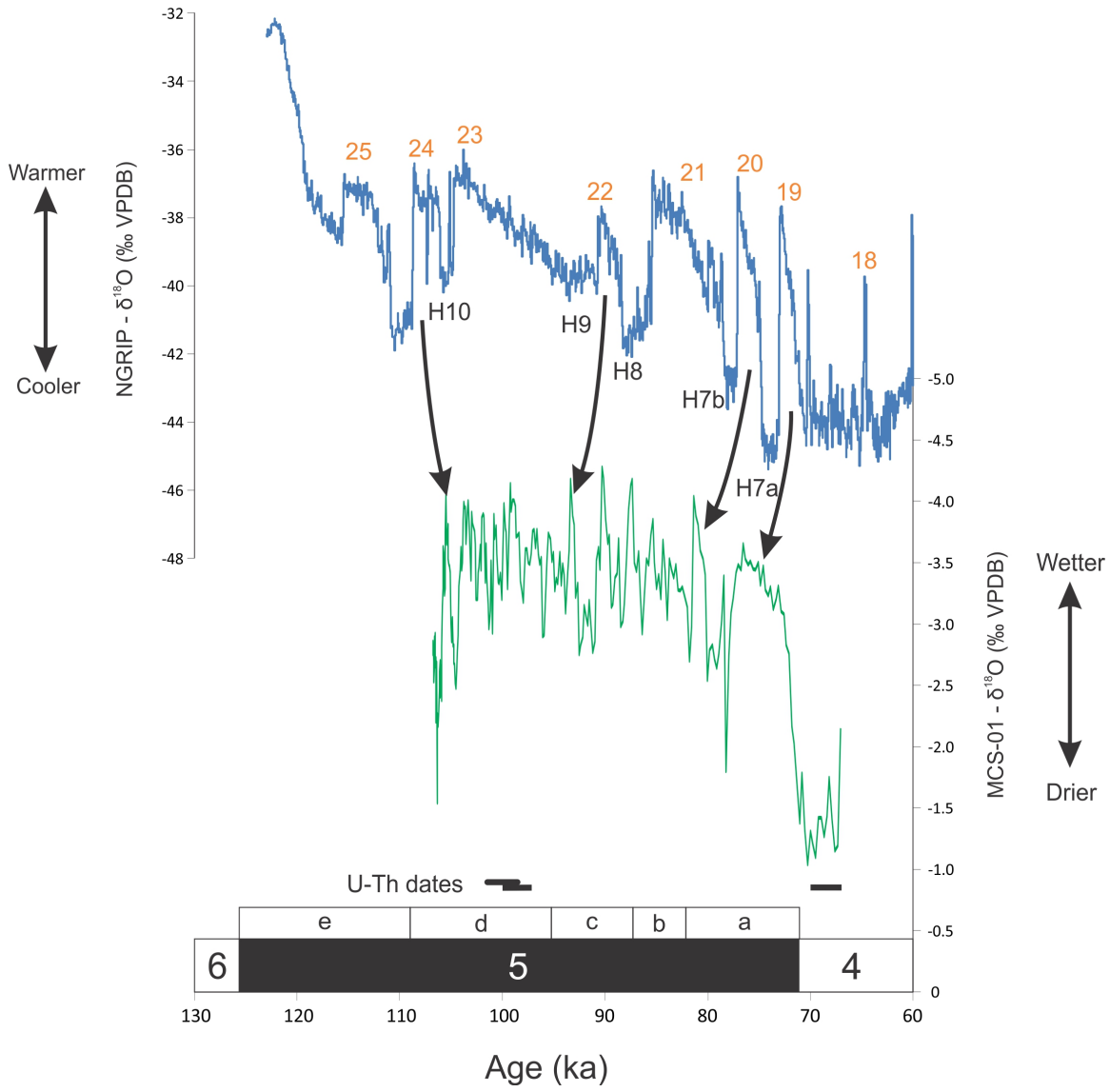

Figure 13: Oxygen isotope data from stalagmite MCS-01 (green) plotted against oxygen isotope data from NGRIP Ice Core (Greenland; blue; Inger et al., 2014)). DO cycles (orange numbers) and Henrich events (black numbers) are also recorded on this figure and represent warm/wet and cold/dry events respectively. The black arrows point to common D-O events (DO events 24, 22, 20, and 19) in both the NGRIP and MCS-01 data. Marine isotope stages shown at the bottom.

Chapter 3- Summary of contributions

3.1 Summary of findings

Stalagmite Majaguas Cave (MCS-01) was collected in the "Salon de la Permencia" (bedroom hall) of the Majaguas Cave, which is part of the Majaguas-Cantera Cave System (22° 23' N, 83° 58' W). The Majagus-Canteras Cave system is found in Pinar del Rio Province, which is located on the western end of the island. Pinar del Rio Province contains one of Cuba's main mountain ranges – the Cordillera de Guaniguanico. The Majaguas-Cantera Cave System lies in the karst of the Sierra de San Carlos, which are part of the Sierra de los Organos mountain range.

Uranium/Thorium dating was used and analyzed via MC-ICP-MS. The dates were taken at the top and bottom of the stalagmite and also above and below the hiastus' in order to constrain the length. Stable isotope samples were analyzed approximately every millimeter to establish the highest possible resolution for this record. Using the 7 U/Th dates, three different age models were developed based on the data. The earliest three dates were modeled using a second-order polynomial and indicate that the growth between 100-68 ka was curvilinear and slowed with time. The second age model that was produced was from the second period of growth which ranged from ~11.0-10.5 ka and was modeled using a linear fit as there were only two dates for this section. For the most recent section of the stalagmite, the growth appears to have begun approximately 400 +/- 70 years ago. Assuming the stalagmite was active when it was collected, as has been reported, the end of the stalagmite corresponds to the present. A liner fit was also used in this section of the stalagmite to assign ages to the stable isotopes.

Although the hiatus are well dated, the limited number of dates between hiatuses means that the chronology of the $\delta^{18}O$ values must be considered provisional. The results from the MCS-01 record have few similarities to the Cuba Medio record established by Warken et al. 2019. The most interesting pattern is found in the oldest section of MCS-01 at 68ka where the first hiatus occurs, and Warken et al. record starts. In this time period the $\delta^{18}O$ of MCS-01 has values of approximately -2 ‰, and the section of the Cuba Medio speleothem record beginning at this time has values of -2 ‰.

Stalagmite MCS-01 is also thought to record northern latitude climatic changes. The data recorded in MCS-01 shows the periodicity found in the NGRIP ice core data. This is noted in two different areas throughout the stalagmite at ~82ka and between 78-70 ka.

As time progresses towards the Holocene, there is a sudden change in $\delta^{18}O$ and $\delta^{13}C$ towards more negative values at the beginning of hiatus 2, around 10.5 ka. This onset of dry conditions in the cave is believed to be a local signal as opposed to a real climatic signal.

1. *Can this stalagmite be used for paleoclimate reconstruction?*
    - Proved it is useful for a paleoclimate reconstruction
    - Able to successfully date 7 samples and extract 363 samples for stable isotopic analysis

- Able to interpret the data and compare it with other studies in the area allowing us to draw conclusions regarding regional and global scale climate patterns

2. *Which known Pleistocene climate events can be identified through geochemical analysis of the speleothem?*
    - A wet phase in the late Pleistocene – MIS 5c
    - The first hiatus at 68 ka is correlated with a study showing a drop in SSTs during the early MIS4 stage
3. *Are other climatic changes, such as precipitation variability and droughts recorded in the Western Cuba region?*
    - When compared to the Cuba Medio study Warken el al. found that more negative $\delta^{18}O$ values occur during MIS 5, which is consistent with MCS-01.
    - This record also shows relatively positive $\delta^{18}O$ values ranging from -1.5‰ during the last glacial period after the early MIS 4 (65 ka) where MCS-01 terminates
    - The biggest difference between these records is the fact that Cuba Medio is active after 68 ka and MCS-01 is not.

3.2 Limitations of the study

Although, like any proxy archive, speleothems do have limitations. For example, sometimes interpretations are unduly speculative or too simplistic in terms of attributing a climatic explanation to the change in the speleothem record, as factors other than climate

(such as vegetation), can be important at determining speleothem chemistry (Fairchaild et al. 2012). In addition, some speleothems can contain hiatuses, as seen in MCS-01, which can relate to dry periods in the cave environment, or other processes. After analyzing both the strengths and weakness of speleothem studies one of the major steps that need to be taken in this field is a more sophisticated understanding of how speleothem records contribute to understanding climate drivers and tele-connections of climate (Fairchild et al. 2012). As well, continued development of new types of proxy and the more effective use of multiproxy approaches need to be considered (Fairchild et al. 2012).

Other limitations in this study include the lack of dates; if more dating was able to be completed this study could be the oldest highest resolution study in the area. The lack of cave monitoring knowledge, is another limitation. Data interpretations could be more precise if more information was known about the specifics of the cave. This would help interpret information more accurately as to differentiate regional vs. northern climatic signals.

3.3 Future work

Although this study provides the most detailed early Pleistocene stable isotope reconstruction study from the region, there remains unanswered questions as the basis of future work.

- More dating completed in order to constrain a better time series analysis of the site. This would enable a further understanding of the environment in relation to the precipitation record and create a higher resolution study.

- A cave monitoring system would also allow for more local information to be observed around the study site. This may help with the interpretation of the overall climate patters observed.
- A second stalagmite study from the same cave would allow for this results to be verified and allow more insight to be found out surrounding the hiatuses that were detected in MCS-01 as to if these events were only noticed in this stalagmite or the cause of these hiatuses were noticed on a more regional setting.

This study provided a unique opportunity to study the early Pleistocene and its response to precipitation patterns in the Caribbean. The stable isotopic analysis allowed us to examine climatic events that were globally detected and recorded subsequently recorded in a Caribbean speleothem to further help us understand these events.

References

Agosta, A. (2010). Preservation and diagenesis in ancient speleothems: evidence from Bear Cave, Yukon Territory. (Master's Thesis). University of Ottawa, Canada.

Banner, J. L., Musgrove, M., and Capo, R., 1994, Tracing ground-water evolution in a limestone aquifer using Sr isotopes: Effects of multiple sources of dissolved ions and mineral-solution reactions: Geology, v. 22, p. 687–690.

Behl, R.J., Kennett, J.P., 1996. Brief interstadial events in the Santa Barbara basin, NE Pacific, during the past 60 kyr. Nature 379, 243–246.

https://doi.org/10.1038/379243a0

Bradbury, J.P., 1989. Late Quaternary lacustrine paleoenvironments in the Cuencaxde Mexico. Quaternary Science Reviews 8, 75}100.

Brown, R.B., 1985. A summary of late-quaternary pollen records from Mexico west of the Isthmus of Tehuantepec. In: Bryant, V.M., Holloway, R.G. (Eds.), Pollen Records of Late Quaternary North American Sediments. American Association of Stratigraphic Palynologists, pp. 71}93.

Dorale, J.A., n.d. Limitations of the Hendy test Criteria in judging the paleoclimatic sutiability of speleothems and the need for replication 8.

Dreybrodt, W., 2012. Speleothem Deposition. In 'Encyclopedia of Caves'. Elsevier, pp. 769–777. https://doi.org/10.1016/B978-0-12-383832-2.00112-2

Fairchild, I.J., Baker, A., & Asrat, A. (2012). Speleothem science: from process to past environemtns. Oxford:Wiley-Blackwell.

Fairchild, I.J., Smith, C.L., Baker, A., Fuller, L., Spotl, C, Mattey, D., McDermott, F,, and E.I.M.F., 2006. Modification and preservation of environmental signals in speleothems, Earth Science Reviews, 75: 105- 153.

Fairchild, I.J. and McMillan, E.A., 2007. Speleothem as indicators of wet and dry periods. International Journal of Speleology, 36(2): 69-74.

Fairchild, I.J., and Treble, P.C., 2009. Trace elements in speleothem as recorders of environmental change, Quaternary Science Reviews, 28: 449-468.

Fensterer, C., Scholz, D., Hoffmann, D., Spötl, C., Pajón, J.M., Mangini, A., 2012. Cuban stalagmite suggests relationship between Caribbean precipitation and the Atlantic Multidecadal Oscillation during the past 1.3 ka. The Holocene 22, 1405–1412. https://doi.org/10.1177/0959683612449759

Fensterer, C., Scholz, D., Hoffmann, D.L., Spötl, C., Schröder-Ritzrau, A., Horn, C., Pajón, J.M., Mangini, A., 2013a. Millennial-scale climate variability during the last 12.5ka recorded in a Caribbean speleothem. Earth and Planetary Science Letters 361, 143–151. https://doi.org/10.1016/j.epsl.2012.11.019

Fensterer, C. (2011). Holocene Caribbean Climate Variability reconstructed from

Speleothems from Western Cuba. (PhD. Thesis). University of Heidelberg, Germany.

Fensterer, C., Scholz, D., Hoffmann, D.L., Spötl, C., Schröder-Ritzrau, A., Horn, C., Pajón, J.M., Mangini, A., 2013b. Millennial-scale climate variability during the last 12.5ka recorded in a Caribbean speleothem. Earth and Planetary Science Letters 361, 143–151. https://doi.org/10.1016/j.epsl.2012.11.019

Ford, D., Williams, P. 2007. Karst Hydrogeology and Geomorphology. West Sussex, England: John Wiley and Sons Ltd.

Frappier, A.B., Sahagian, D., Carpenter, S.J., González, L.A., Frappier, B.R., 2007. Stalagmite stable isotope record of recent tropical cyclone events. Geology 35, 111. https://doi.org/10.1130/G23145A.1

Greene, C.H., Pershing, A.J., Cronin, T.M., Ceci, N., 2008 Arctic Climate Change and its impacts on the ecology of the North Atlantic. Ecology 89, S24-S38. https://doi.org/10.1890/07-0550.1

Gregory, B.R.B., Peros, M., Reinhardt, E.G., Donnelly, J.P., 2015. Middle–late Holocene Caribbean aridity inferred from foraminifera and elemental data in sediment cores from two Cuban lagoons. Palaeogeography, Palaeoclimatology, Palaeoecology 426, 229–241. https://doi.org/10.1016/j.palaeo.2015.02.029

Grimm, E., G. L. Jacobson Jr., W. A. Watts, B. C. S. Hansen, and K. A. Maasch (1993). 50,000-year record of climate oscillations from Florida and its temporal correlation with the Heinrich events. Science, Vol. 216, 198–200.

Grimm, E.C., Watts, W.A., Jacobson Jr., G.L., Hansen, B.C.S., Almquist, H.R., Dieffenbacher-Krall, A.C., 2006. Evidence for warm wet Heinrich events in Florida. Quaternary Science Reviews 25, 2197–2211. https://doi.org/10.1016/j.quascirev.2006.04.008

Harmon, R.S., Schwarcz, H.P., Gascoyne, M., Hess, J.W. and Ford, D.C., 2007. Paleoclimate information from speleothems: The present as a guide to the past. In Studies of Cave Sediments - Physical and Chemical Records of Paleoclimate. Kluwer Academic, New York, p. 199-226.

Haug, G.H., 2001. Southward Migration of the Intertropical Convergence Zone Through the Holocene. Science 293, 1304–1308. https://doi.org/10.1126/science.1059725

Haug, G. H., D. Gu¨nther, L. C. Peterson, D. M. Sigman, K. A. Hughen, and B. Aeschlimann (2003). Climate and the Collapse of Maya Civilization. Science, Vol. 299, 1731.

Hendy, C. H. (1971). The isotopic geochemistry of speleothems - I. The calculation of the effects of different modes of formation on the isotopic composition of

speleothems and their applicability as paleoclimatic indicators. Geochimica et Cosmochimica Acta, Vol. 35, 801–824.

van Hengstum, P.J., Maale, G., Donnelly, J.P., Albury, N.A., Onac, B.P., Sullivan, R.M., Winkler, T.S., Tamalavage, A.E., MacDonald, D., 2018. Drought in the northern Bahamas from 3300 to 2500 years ago. Quaternary Science Reviews 186, 169–185. https://doi.org/10.1016/j.quascirev.2018.02.014

Hill, C.A. and Forti, P. 2004. 'Speleothems: Carbonate', p. 690, Encyclopedia of Caves and Karst Science. New York.

Hodell, D., J. H. Curtis, G. A. Jones, A. Higuera-Gundy, M. Brenner, M. W. Binford, and K. T. Dorsey (1991). Reconstruction of Caribbean climate change over the past 10,500 years. Nature, Vol. 352, 790–793.

Hodell, D., J. H. Curtis, and M. Brenner (1995). Possible role of climate in the collapse of Classic Maya civilization. Nature, Vol. 375, 391–394.

Hopley, P.H., Marshall, J.D., Weedon, G.P., Latham, A.G., Herries, A. and Kuykendall, K.L., 2007. Oribital forcing and the spread of C4 grasses in the late Neogene: stable isotope evidence from South African speleothems, Journal of Human Evolution, 53:620-634

Inger K. Seierstad, Peter M. Abbott, Matthias Bigler, Thomas Blunier, Anna J.

Bourne, Edward Brook, Susanne L. Buchardt, Christo Buizert, Henrik B. Clausen, Eliza Cook, Dorthe Dahl-Jensen, Siwan M. Davies, Myriam Guillevic, Sigfús J. Johnsen, Desirée S. Pedersen, Trevor J. Popp, Sune O. Rasmussen, Jeffrey P. Severinghaus, Anders Svensson and Bo M. Vinther, Consistently dated records from the Greenland GRIP, GISP2 and NGRIP ice cores for the past 104 ka reveal regional millennial-scale δ18O gradients with possible Heinrich event imprint, Quaternary Science Reviews, 10.1016/j.quascirev.2014.10.032, 106, (29-46), (2014).

Lachniet, M.S., 2009. Climatic and environmental controls on speleothem oxygen-isotope values. Quaternary Science Reviews 28, 412–432. https://doi.org/10.1016/j.quascirev.2008.10.021

Lachniet, M.S., 2004. A 1500-year El Niño/Southern Oscillation and rainfall history for the Isthmus of Panama from speleothem calcite. Journal of Geophysical Research 109. https://doi.org/10.1029/2004JD004694

Lane CS, Horn SP, Mora CI, Orvis KH. 2009. Late-Holocene paleoenvironmental change at mid-elevation on the Caribbean slope of the Cordillera Central, Dominican Republic: a multi-site, multi-proxy analysis. Quaternary Science Reviews. 28: 2239–2260.

Lane, C.S., Horn, S.P., Orvis, K.H., Thomason, J.M., 2011. Oxygen isotope evidence of Little Ice Age aridity on the Caribbean slope of the Cordillera Central, Dominican Republic. Quaternary Research 75, 461–470.

https://doi.org/10.1016/j.yqres.2011.01.002

Lane, C.S., Horn, S.P., Kerr, M.T., 2014. Beyond the Mayan Lowlands: impacts of the Termi- nal Classic Drought in the Caribbean Antilles. Quat. Sci. Rev. 86, 89–98.

Leduc, G., Vidal, L., Tachikawa, K., Rostek, F., Sonzogni, C., Beaufort, L., Bard, E., 2007. Moisture transport across Central America as a positive feedback on abrupt climatic changes. Nature 445, 908–911. https://doi.org/10.1038/nature05578

Lee, J.-E., Swann, A.L., 2010. Evaluation of the "amount effect" at speleothem sites in the Asian monsoon region. IOP Conference Series: Earth and Environmental Science 9, 012023. https://doi.org/10.1088/1755-1315/9/1/012023

Little, M.G., Schneider, R.R., Kroon, D., Price, B., Summerhayes, C.P., Segl, M., 1997. Trade wind forcing of upwelling, seasonally, and Heinrich events as a response to sub-Milankovitch climate variability. Paleoceanography 12, 568–576. https://doi.org/10.1029/97PA00823

Lozano-Garcia, M. d. S., Caballero, M., Ortega, B., Rodriguez, A., Sosa, S., 2007. Tracing the effects of the Little Ice Age in the tropical lowlands of eastern Mesoamerica. Proceedings of the National Academy of Sciences 104, 16200–16203. https://doi.org/10.1073/pnas.0707896104

Marshall, S.J., Koutnik, M.R., 2006. Ice sheet action versus reaction: Distinguishing

between Heinrich events and Dansgaard-Oeschger cycles in the North Atlantic: MILLENNIAL-SCALE IRD VARIABILITY. Paleoceanography 21, n/a-n/a. https://doi.org/10.1029/2005PA001247

McDermott, F., 2004. Palaeo-climate reconstruction from stable isotope variations in speleothems: a review. Quaternary Science Reviews 23, 901–918. https://doi.org/10.1016/j.quascirev.2003.06.021

Medina-Elizalde, M., Burns, S.J., Lea, D.W., Asmerom, Y., von Gunten, L., Polyak, V., Vuille, M., Karmalkar, A., 2010. High resolution stalagmite climate record from the Yucatán Peninsula spanning the Maya terminal classic period. Earth and Planetary Science Letters 298, 255–262. https://doi.org/10.1016/j.epsl.2010.08.016

Metcalfe, S.E., O'Hara, S.L., Caballero, M., Davies, S.J., 2000. Records of Late Pleistocene–Holocene climatic change in Mexico — a review. Quaternary Science Reviews 19, 699–721. https://doi.org/10.1016/S0277-3791(99)00022-0

Pajón JM, Hernández I, Ortega F, Macle J. 2001. Periods of wet climate in Cuba: evaluation of expression in karst of Sierra de San Carlos. In: Markgraf V,

editor. Interhemispheric Climate Linkages. San Diego (CA): Academic Press. p. 217–226

Pajón JM, Curtis J, Tudhope S, Metcalfe S, Brenner M, Guilderson T, Chicott C, Grimm E, Hernández I. 2006. Isotope records from a stalagmite from Dos Anas cave in Pinal Del Rio Provience, Cuba. Palaeoclimatic Implications. International Symposium on Nuclear & Related Techniques. Havana, Cuba.

Palmer, A. N. 2007. Cave Geology. Dayton, OH: Cave Books. p. 1-37

Peros MC, Reinhardt EG, Schwarcz HP, Davis AM. 2007b. High-resolution paleosalinity reconstruction from Laguna de la Leche, north coastal Cuba, using Sr, O, and C isotopes. Palaeogeography, Palaeoclimatology, Palaeoecology. 245: 535–550.

Peros MC, Gregory B, Matos F, Reinhardt E, Desloges J. 2015. Late-Holocene record of lagoon evolution, climate change, and hurricane activity from southeastern Cuba. The Holocene. 25:1483–1497.

Peros, M., Collins, S., G'Meiner, A.A., Reinhardt, E., Pupo, F.M., 2017. Multistage 8.2 kyr event revealed through high-resolution XRF core scanning of Cuban sinkhole sediments: Sinkhole Sediments Reveal 8.2 kyr Event. Geophysical Research Letters 44, 7374–7381. https://doi.org/10.1002/2017GL074369

Ponte, J.M., Font, E., Veiga-Pires, C., Hillaire-Marcel, C., Ghaleb, B., 2017. The effect of

speleothem surface slope on the remanent magnetic inclination: Speleothem Shape and Magnetism. Journal of Geophysical Research: Solid Earth 122, 4143–4156. https://doi.org/10.1002/2016JB013789

Scholz, D., Mühlinghaus, C., Mangini, A., 2009. Modelling δ13C and δ18O in the solution layer on stalagmite surfaces. Geochimica et Cosmochimica Acta 73, 2592–2602. https://doi.org/10.1016/j.gca.2009.02.015

Trouet, V.R., Esper, J., Graham, N.E., Baker, A., Scourse, J.D., and Frank, D.C., 2009, Persistent positive North Atlantic Oscillation mode dominated the Medieval Climate Anomaly: Science, v. 324, p. 78–80, doi:10.1126/science.1166349.

Turgeon, S.C. and Lundberg, J., 2007. Establishing a speleothem chronology for southwestern Oregon. In Studies of Cave Sediments - Physical and Chemical Records ofPaleoclimate. Kluwer Academic, New York, p. 273-302.

Van Beynen, P., Bourbonniere, R., Ford, D. and Schwarcz, H., 2001. Causes of colour and fluorescence in speleothem. Chemical Geology, 175: 319-341.

White, W.B., 2007. Paleoclimate records from speleothem in limestone caves. In Studies of Cave Sediments — Physical and Chemical Records of Paleoclimate. Kluwer Academic, New York, p.

135-175.

Appendix

Sample	$[^{238}U]$ ppb	±	$[^{232}Th]$ ppb	±	$(^{234}U/^{238}U)$	±	$(^{230}Th/^{234}U)$	±	$(^{230}Th/^{238}U)$	±	$(^{234}U/^{232}Th)$	±	$(^{238}U/^{232}Th)$	±	$(^{230}Th/^{232}Th)$	±	$^{230}Th/U$ age ka	±	$(^{234}U/^{238}U)_0$	±
MCS-1	115.070	0.615	0.873	0.004	1.451	0.009	0.628	0.009	0.912	0.013	584.951	3.912	403.055	2.957	367.390	5.510	100.545	2.550	1.600	0.011
MCS-2	192.968	1.775	8.644	0.177	1.458	0.014	0.479	0.007	0.699	0.012	99.494	2.139	68.231	1.534	47.705	1.215	68.222	1.803	1.556	0.016
MCS-3	125.819	1.161	1.325	0.006	1.328	0.013	0.097	0.002	0.129	0.002	385.526	3.134	290.263	3.029	37.300	0.689	11.022	0.250	1.339	0.013
MCS-4	123.947	1.107	1.532	0.007	1.329	0.013	0.093	0.002	0.123	0.003	328.546	2.569	247.258	2.483	30.506	0.622	10.557	0.257	1.339	0.013
MCS-5	128.601	1.113	0.134	0.003	1.320	0.013	0.004	0.001	0.005	0.001	3881.056	103.965	2940.720	80.823	14.554	2.509	0.409	0.070	1.320	0.013
MCS-6	107.159	0.956	0.676	0.005	1.302	0.013	n.d	n.d	n.d.	n.d.	630.797	6.213	484.645	5.666	n.d.	n.d.	n.d.	n.d..	n.d.	n.d.
MCS-7	115.598	0.650	1.049	0.012	1.467	0.015	0.621	0.009	0.912	0.011	494.222	7.578	336.787	4.220	307.106	5.151	98.752	2.554	1.618	0.018

Sample Number	Depth (mm)	δ13C	δ18O
1	1	-4.61	-2.79
2	2.07438017	-5.56	-2.75
3	3.14876034	-5.89	-2.86
4	4.22314051	-5.45	-2.7
5	5.29752068	-4.52	-2.53
6	6.37190085	-4.14	-2.66
7	7.44628102	-4.98	-2.89
8	8.52066119	-5.2	-2.79
9	9.59504136	-5.62	-2.92
10	10.66942153	-5.6	-2.65
11	11.7438017	-6.54	-2.72
12	12.81818187	-6.44	-2.2
13	13.89256204	-6.23	-2.66
14	14.96694221	-5.65	-2.69
15	16.04132238	-5.84	-1.54
16	17.11570255	-4.4	-2.27
17	18.19008272	-3.89	-2.23
18	19.26446289	-2.33	-2.17
19	20.33884306	-2.29	-2.29
20	21.41322323	-2.4	-2.47
21	22.4876034	-2.64	-2.61
22	23.56198357	-2.89	-2.7
23	24.63636374	-3.45	-2.41
24	25.71074391	-3.62	-2.66
25	26.78512408	-2.69	-2.38
26	27.85950425	-5.29	-2.81
27	28.93388442	-5.28	-3.15
28	30.00826459	-6.45	-3.29
29	31.08264476	-7.23	-3.63
30	32.15702493	-8	-3.58
31	33.2314051	-7.22	-3.24
32	34.30578527	-7.39	-3.29
33	35.38016544	-7.84	-3.75
34	36.45454561	-9.1	-4.05
35	37.52892578	-7.19	-3.65
36	38.60330595	-8.07	-3.71
37	39.67768612	-9.11	-3.81
38	40.75206629	-8.7	-3.53
39	41.82644646	-8.18	-3.49
40	42.90082663	-7.88	-3.47
41	43.9752068	-8.33	-3.42
42	45.04958697	-5.84	-3.01

43	46.12396714	-6.64	-2.86
44	47.19834731	-6.39	-3.05
45	48.27272748	-4.92	-2.82
46	49.34710765	-5.43	-2.83
47	50.42148782	-4.53	-2.68
48	51.49586799	-4.6	-2.67
49	52.57024816	-3.57	-2.52
50	53.64462833	-3.18	-2.48
51	54.7190085	-4.44	-2.61
52	55.79338867	-4.49	-2.78
53	56.86776884	-4.85	-2.91
54	57.94214901	-6.01	-3.31
55	59.01652918	-5.53	-3.44
56	60.09090935	-5.93	-3.62
57	61.16528952	-7.35	-3.44
58	62.23966969	-7.7	-3.5
59	63.31404986	-8.39	-3.85
60	64.38843003	-8.47	-3.99
61	65.4628102	-8.52	-3.95
62	66.53719037	-8.73	-3.95
63	67.61157054	-7.4	-3.66
64	68.68595071	-8.17	-3.92
65	69.76033088	-8.52	-4
66	70.83471105	-8.22	-3.88
67	71.90909122	-8.07	-3.72
68	72.98347139	-6.45	-3.36
69	74.05785156	-7.79	-3.91
70	75.13223173	-7.56	-3.82
71	76.2066119	-8.41	-3.8
72	77.28099207	-7.96	-3.76
73	78.35537224	-7.58	-3.65
74	79.42975241	-5.35	-3.2
75	80.50413258	-6.14	-3.2
76	81.57851275	-6.72	-3.42
77	82.65289292	-6.15	-3.46
78	83.72727309	-7.1	-3.64
79	84.80165326	-6.69	-3.44
80	85.87603343	-7.47	-3.87
81	86.9504136	-7.78	-3.9
82	88.02479377	-8.08	-3.88
83	89.09917394	-6.01	-3.34
84	90.17355411	-7.44	-3.65
85	91.24793428	-7.05	-3.37

86	92.32231445	-5.93	-3.16
87	93.39669462	-3.55	-2.96
88	94.47107479	-5.16	-3.11
89	95.54545496	-5.88	-3.51
90	96.61983513	-4.4	-2.93
91	97.6942153	-7.77	-3.89
92	98.76859547	-7.3	-3.7
93	99.84297564	-8.59	-3.8
94	100.9173558	-7.47	-3.57
95	101.991736	-5.9	-3.34
96	103.0661162	-5.42	-3.33
97	104.1404963	-7.05	-3.41
98	105.2148765	-5.41	-3.2
99	106.2892567	-5.65	-3.47
100	107.3636368	-7.91	-3.98
101	108.438017	-7.85	-3.78
102	109.5123972	-7.61	-3.75
103	110.5867773	-5.78	-3.29
104	111.6611575	-6.74	-3.72
105	112.7355377	-8.74	-4.14
106	113.8099179	-8.81	-3.92
107	114.884298	-8.67	-4.01
108	115.9586782	-8.83	-4.01
109	117.0330584	-8.21	-3.96
110	118.1074385	-7.48	-3.71
111	119.1818187	-7.27	-3.72
112	120.2561989	-7.61	-3.74
113	121.330579	-5.7	-3.35
114	122.4049592	-5.19	-3.27
115	123.4793394	-4.59	-3.18
116	124.5537196	-6.61	-3.34
117	125.6280997	-7.64	-3.61
118	126.7024799	-7.76	-3.61
119	127.7768601	-8.03	-3.5
120	128.8512402	-7.33	-3.49
121	129.9256204	-8.04	-3.57
122	131.0000006	-8.37	-3.76
123	132.0743807	-7.61	-3.77
124	133.1487609	-7.8	-3.62
125	134.2231411	-8.28	-3.77
126	135.2975213	-7.14	-3.57
127	136.3719014	-7.2	-3.49
128	137.4462816	-7.39	-3.54

129	138.5206618	-5.4	-2.9
130	139.5950419	-4.87	-2.91
131	140.6694221	-5.43	-3.21
132	141.7438023	-6.68	-3.52
133	142.8181824	-7.06	-3.74
134	143.8925626	-6.46	-3.69
135	144.9669428	-6.81	-3.51
136	146.041323	-7.28	-3.58
137	147.1157031	-6.22	-3.27
138	148.1900833	-7.61	-3.37
139	149.2644635	-7.27	-3.33
140	150.3388436	-7.16	-3.58
141	151.4132238	-7.11	-3.32
142	152.487604	-6.27	-3.49
143	153.5619841	-7.26	-3.4
144	154.6363643	-5.76	-3.09
145	155.7107445	-6.65	-3.41
146	156.7851247	-6.38	-3.6
147	157.8595048	-8.2	-4.18
148	158.933885	-7.7	-3.88
149	160.0082652	-7.01	-3.81
150	161.0826453	-5.74	-3.22
151	162.1570255	-6.61	-3.33
152	163.2314057	-2.97	-2.75
153	164.3057858	-4.41	-2.83
154	165.380166	-4.66	-2.89
155	166.4545462	-4.17	-3.15
156	167.5289264	-4.56	-3.05
157	168.6033065	-4.99	-2.99
158	169.6776867	-4.76	-3.19
159	170.7520669	-3.68	-2.94
160	171.826447	-4.65	-2.77
161	172.9008272	-5.06	-2.86
162	173.9752074	-7.72	-3.52
163	175.0495875	-8.28	-3.62
164	176.1239677	-7.52	-3.45
165	177.1983479	-9.13	-4.28
166	178.2727281	-8.79	-4.19
167	179.3471082	-8.11	-3.85
168	180.4214884	-8	-3.66
169	181.4958686	-8.57	-3.72
170	182.5702487	-6.23	-3.14
171	183.6446289	-6.44	-3.16

172	184.7190091	-6.51	-3.38
173	185.7933892	-6.89	-3.41
174	186.8677694	-7.43	-3.69
175	187.9421496	-4.28	-2.98
176	189.0165298	-4.77	-3.02
177	190.0909099	-5.23	-3.16
178	191.1652901	-6.2	-3.52
179	192.2396703	-7.45	-3.93
180	193.3140504	-8.55	-4.13
181	194.3884306	-8.79	-4.18
182	195.4628108	-7.7	-3.5
183	196.5371909	-6.77	-3.43
184	197.6115711	-7.15	-3.59
185	198.6859513	-5.9	-3.29
186	199.7603315	-4.28	-2.92
187	200.8347116	-6.09	-3.23
188	201.9090918	-7.74	-3.53
189	202.983472	-7.39	-3.48
190	204.0578521	-7.7	-3.72
191	205.1322323	-7.72	-3.85
192	206.2066125	-6.59	-3.5
193	207.2809926	-5.99	-3.29
194	208.3553728	-6.08	-3.4
195	209.429753	-6.52	-3.21
196	210.5041332	-6.66	-3.68
197	211.5785133	-5.63	-3.43
198	212.6528935	-5.25	-3.04
199	213.7272737	-7.09	-3.53
200	214.8016538	-7.16	-3.44
201	215.876034	-7.17	-3.38
202	216.9504142	-6.87	-3.48
203	218.0247943	-6.41	-3.28
204	219.0991745	-6.5	-3.27
205	220.1735547	-6.11	-3.3
206	221.2479349	-6.69	-3.23
207	222.322315	-6.26	-3.14
208	223.3966952	-4.04	-2.7
209	224.4710754	-3.67	-2.98
210	225.5454555	-7.43	-4.04
211	226.6198357	-8.21	-3.88
212	227.6942159	-8.2	-3.81
213	228.768596	-6.83	-3.6
214	229.8429762	-6.71	-3.53

215	230.9173564	-6.54	-3.4
216	231.9917366	-4.66	-2.54
217	233.0661167	-4.88	-2.79
218	234.1404969	-5.97	-2.83
219	235.2148771	-5.37	-2.71
220	236.2892572	-5.06	-2.64
221	237.3636374	-4.98	-2.76
222	238.4380176	-6.34	-3.03
223	239.5123977	-7.71	-3.39
224	240.5867779	-7.6	-1.8
225	241.6611581	-6.12	-2.74
226	242.7355383	-7.02	-3.09
227	243.8099184	-7.13	-3.21
228	244.8842986	-7.26	-3.42
229	245.9586788	-7.55	-3.48
230	247.0330589	-7.29	-3.44
231	248.1074391	-7.81	-3.65
232	249.1818193	-8.42	-3.53
233	250.2561994	-7.88	-3.48
234	251.3305796	-7.79	-3.51
235	252.4049598	-7.92	-3.45
236	253.47934	-7.86	-3.44
237	254.5537201	-7.76	-3.5
238	255.6281003	-7.65	-3.32
239	256.7024805	-7.91	-3.47
240	257.7768606	-7.95	-3.28
241	258.8512408	-7.71	-3.23
242	259.925621	-7.74	-3.3
243	261.0000011	-5.5	-3.12
244	262.0743813	-5.41	-3.2
245	263.1487615	-5.57	-3.31
246	264.2231417	-5.7	-3.1
247	265.2975218	-6.17	-3.08
248	266.371902	-6.4	-2.83
249	267.4462822	-5.89	-2.76
250	268.5206623	-10.56	-2.16
251	269.5950425	-11.88	-2.03
252	270.6694227	-11.28	-1.7
253	271.7438028	-9.94	-1.38
254	272.818183	-11.35	-1.78
255	273.8925632	-9.93	-1.32
256	274.9669434	-9.47	-1.04
257	276.0413235	-9.37	-1.31

258	277.1157037	-9.28	-1.21
259	278.1900839	-8.72	-1.1
260	279.264464	-9.04	-1.42
261	280.3388442	-8.67	-1.42
262	281.4132244	-8.18	-1.27
263	282.4876045	-8.28	-1.43
264	283.5619847	-9.32	-1.75
265	284.6363649	-8.86	-1.41
266	285.7107451	-8.11	-1.15
267	286.7851252	-7.9	-1.19
268	287.8595054	-10.7	-2.15
269	288.9338856	-12.73	-3.28
270	290.0082657	-12.71	-2.8
271	291.0826459	-12.5	-2.88
272	292.1570261	-12.85	-3.36
273	293.2314062	-12.43	-2.45
274	294.3057864	-12.59	-2.9
275	295.3801666	-11.32	-2.92
276	296.4545468	-11.88	-2.98
277	297.5289269	-12.46	-2.96
278	298.6033071	-12.23	-2.61
279	299.6776873	-10.15	-2.12
280	300.7520674	-10.07	-2.14
281	301.8264476	-8.8	-1.84
282	302.9008278	-8.56	-1.55
283	303.9752079	-8.17	-1.39
284	305.0495881	-7.6	-1.8
285	306.1239683	-7.93	-1.79
286	307.1983485	-7.54	-1.67
287	308.2727286	-9.42	-1.93
288	309.3471088	-9.4	-1.94
289	310.421489	-8.11	-1.99
290	311.4958691	-8.15	-1.82
291	312.5702493	-9.6	-2.23
292	313.6446295	-9.2	-2.02
293	314.7190096	-9.1	-2.06
294	315.7933898	-9.05	-1.99
295	316.86777	-8.82	-1.74
296	317.9421502	-8.21	-1.66
297	319.0165303	-8.1	-1.79
298	320.0909105	-7.14	-1.21
299	321.1652907	-7.04	-1.19
300	322.2396708	-6.33	-0.97

301	323.314051	-7.49	-1.14
302	324.3884312	-8.2	-1.37
303	325.4628113	-7.82	-1.39
304	326.5371915	-7.84	-1.14
305	327.6115717	-8.37	-1.1
306	328.6859519	-8.68	-1.36
307	329.760332	-10.18	-1.95
308	330.8347122	-10.12	-2.2
309	331.9090924	-7.42	-1.6
310	332.9834725	-7.36	-1.48
311	334.0578527	-6.98	-1.46
312	335.1322329	-6.66	-1.24
313	336.206613	-8.34	-1.8
314	337.2809932	-6.91	-1.16
315	338.3553734	-5.34	-0.69
316	339.4297536	-5.34	-0.72
317	340.5041337	-5.46	-0.49
318	341.5785139	-6.23	-0.69
319	342.6528941	-6.34	-0.61
320	343.7272742	-6.41	-0.66
321	344.8016544	-6.29	-0.81
322	345.8760346	-4.95	-0.65
323	346.9504147	-4.74	-0.79
324	348.0247949	-3.51	-0.62
325	349.0991751	-3.67	-0.48
326	350.1735553	-3.15	-0.69
327	351.2479354	-4.26	-1.08
328	352.3223156	-4.58	-1.38
329	353.3966958	-4.68	-1.44
330	354.4710759	-4.23	-1.25
331	355.5454561	-3.56	-1.29
332	356.6198363	-3.35	-0.9
333	357.6942164	-3.12	-1.22
334	358.7685966	-3.59	-1.17
335	359.8429768	-4.12	-1.16
336	360.917357	-2.68	-0.86
337	361.9917371	-1.5	-0.78
338	363.0661173	-7.63	-3.76
339	364.1404975	-12.62	-5.25
340	365.2148776	-12.9	-4.7
341	366.2892578	-13	-4.72
342	367.363638	-12.19	-4.56
343	368.4380181	-12.38	-5.04

344	369.5123983	-13.15	-5.72
345	370.5867785	-11.9	-5.09
346	371.6611586	-9.84	-4.07
347	372.7355388	-9.46	-3.47
348	373.809919	-9.29	-3.66
349	374.8842992	-9.41	-3.74
350	375.9586793	-9.53	-3.74
351	377.0330595	-9.87	-3.75
352	378.1074397	-9.74	-3.81
353	379.1818198	-9.82	-3.82
354	380.2562	-9.6	-3.54
355	381.3305802	-8.04	-3.21
356	382.4049603	-7.68	-3.39
357	383.4793405	-9.63	-3.99
358	384.5537207	-9.35	-3.68
359	385.6281009	-7.4	-3.3
360	386.702481	-7.67	-3.45
361	387.7768612	-7.41	-3.28
362	388.8512414	-7.65	-3.54
363	389.9256215	-7.78	-3.79